ENERGY HARVESTING NANOCOATED PIEZOCERAMICS FOR LOW POWER SYSTEMS

A Thesis
presented in partial fulfillment of requirements
for the degree of Master's of Science
in the Department of Mechanical Engineering
The University of Mississippi

By

Quinten M. Humphrey

May 2018

ABSTRACT

There has become a tremendous increase in the interest of alternative energy sources due to the dwindling of fossil fuels. One such renewable energy resource is mechanical vibrations. These vibrations can occur in a variety of places such as streets, highways and railways due to vehicle traffic, sidewalks and dance floors due to foot traffic, and manufacturing facilities due to their instability of their machines, just to name a few. The utilization of piezoelectric ceramics is moving to the forefront of harvesting energy from vibrations.

In the research being conducted in this study, a lead zirconate titanate (PZT) ceramic disk was applied to a fixed-free cantilever beam. Several nanocoatings were developed in this research and tested to determine their impact on improving the ability of the traditional piezoelectric ceramic to harvest the energy from vibrations. Three nanocoating mixtures were developed using three types of nanoparticles: barium titanate, zinc oxide, and strontium titanate. The results show that the zinc oxide nanoparticle mixture was the most effective in enhancing the PZT ceramic, while strontium titanate showed that it is the best if optimizing the cost.

LIST OF ABBREVIATIONS AND SYMBOLS

D_i – dielectric displacement (N/mV or C/m^2)

ε_k – strain vector

E_j – applied electric field vector (volts/meter)

σ_m – stress vector (N/m^2)

d_{jk}^{c} and d_{im}^{d} – piezoelectric constants (m/V or C/N)

e_{ij}^{σ} - dielectric permittivity (N/V^2 or F/m)

S_{km}^{E}- elastic compliance matric (m^2/N)

x – value of power output for given mixture composition

$x_{reference}$ – value of power output for noncoated piezoelectric

ACKNOWLEDGEMENTS

I would like to express my gratitude towards my advisor, Dr. Tyrus McCarty, for allowing me to further my education in mechanical engineering. Not only has he accepted me into the program, he has assisted me with problems I have come upon and provided solutions to overcome the obstacles. Also, I would like to thank him for the financial support. I sincerely extend thanks to Dr. Jagdish Sharma and to Dr. Waheed Uddin for their important service on my thesis committee. I am grateful for Ms. Janet McBride for handling the order placements. I would like to thank Dinesh Palikhel for his teachings and support in the lab. Furthermore, valuable attributions provided by Matthew Nelms and Damian Stoddard are acknowledged.

DEDICATION

I would like to thank my parents for their continuous support throughout my college career and for pushing me to be the best that I can be.

TABLE OF CONTENTS

LIST OF TABLES

LIST OF FIGURES

1. INTRODUCTION

With fossil fuels being the current source of power, this has caused many problems, such as the threat of pollution throughout the environment. Also, our strong dependence on a nonrenewable, dwindling source of power is detrimental to the future of our society. This has spurred a lot of interest in alternative energy sources that are renewable. Some of these renewable sources include ambient light, ambient radio frequency, thermal waste, and mechanical vibrations. It is also important to note that these renewable sources of energy are clean and eco-friendly.

One of the promising areas of alternative energy is the harvesting of energy from systems that lose energy because of mechanical vibrations. Examples include highways, railways, bridges, factory machinery, vehicles, and many others.

One of the largest application areas for using this harvested energy is the many wireless low power devices that are used in our everyday lives, handheld and wearable devices, and sensors for monitoring things like traffic, integrity of buildings, as well as our health.

There is a growing interest in utilizing piezoelectric ceramics to harvest this vibrational energy. Piezoelectric ceramics have the unique ability of converting mechanical energy, such as vibrations, into electricity. Lead zirconate titanate (PZT) has been the most used ceramic for energy harvesting. A piezoelectric energy harvester is by definition a fixed-free cantilever beam with a piezoceramic attached to it.

At present piezoelectric ceramics like PZTs are only able to extract and output vibrational energy in small amounts. Thus, this research is focused on enhancing the power output of the traditional piezoelectric ceramic PZT for low power systems. Several nanoparticle coatings have

been developed to enhance the power output of this traditional PZT. The basis for using nanoparticles is the fact that some of the key properties of the material become more pronounced on a nanoscale. In addition to nanoparticles, the coating consists of a ferrofluid and a epoxy binder. In this study, three types of nanoparticles are used to develop the coatings, barium titanate, strontium titanate, and zinc oxide.

Chapter 2 gives background detail on the characteristics of piezoelectricity as well as some current applications. Chapter 3 discusses the laboratory setup, while Chapter 4 presents the results and discussion related to the testing of the traditional PZT and the nanocoated PZT. Chapter 5 presents the conclusions and the future work recommendations.

2. THEORY

The purpose for this research is to find a coating mixture that will enhance the power output of a piezoelectric ceramic. This chapter will discuss the background of piezoelectricity, the nanoparticles, ferrofluid, epoxy, and how they are being used for energy harvesting. The overall goal is to implement a way to increase the power output of these low energy producing systems.

2.1 PIEZOELECTRICITY

When a material containing crystalline materials is bent due to mechanical stress, this creates a form of electricity called piezoelectricity. Piezoelectricity was discovered in crystals such as tournmaline, quartz, and Rochelle salt by French physicist brothers, Jacques and Pierre Curie. There are many materials that exhibit piezoelectricity: natural occurring and synthetic crystals, bones, biological materials, ceramics, and polymers. [2]

A piezoelectric crystal is electrically neutral even though the atoms are not symmetrically arranged. This is because the crystal has electric charges which are perfectly balanced meaning that a positive charge is cancelling out a negative charge. When pressure is put onto the crystals, this causes the crystal structure to deform which squeezes or separates the atoms and upsets the balance causing net electrical charges. This creates a linear effect which means that the polarization varies directly with the applied stress. It is also direction dependent, so the compressive and tensile stresses generate electric fields and voltages of opposite polarity. This is called the direct effect. This can be seen in Figure 1.

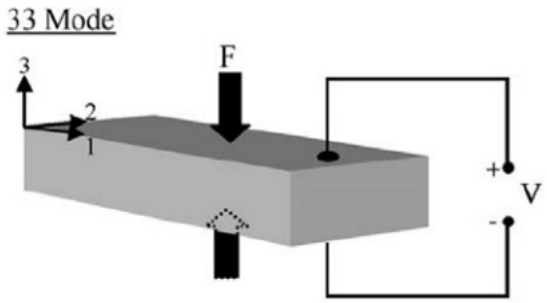

Figure 1: Direct Piezoelectric Effect [38]

Not only can piezoelectric crystals be deformed from pressure, but there is an effect that occurs in the opposite way. It is called the reverse-piezoelectric effect, or converse effect. When a voltage runs across a crystal, the atoms are being exposed to "electrical pressure." The atoms will have to move to rebalance themselves. The will cause the ceramic to have tensile stresses. This can be seen in Figure 2.

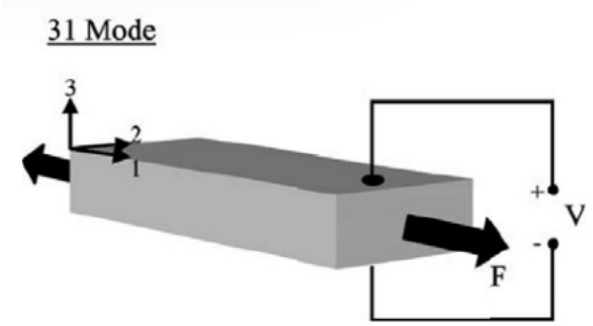

Figure 2: Converse Piezoelectric Effect [38]

These behaviors can be modeled by two linearized constitutive equations. Equations 1 and 2 refer to the direct and converse effect, respectively.

Direct piezoelectric effect:

$$\{D_i\} = [e_{ij}^{\sigma}]\{E_j\} + [d_{im}^{d}]\{\sigma_m\} \qquad (1)$$

Converse piezoelectric effect:

$$\{\varepsilon_k\} = \left[d_{jk}^{c}\right]\{E_j\} + [S_{km}^{E}]\{\sigma_m\} \qquad (2)$$

Where $\{D_i\}$ is the dielectric displacement (N/mV or C/m^2) vector, $\{\varepsilon_k\}$ is the strain vector, E_j is the applied electric field vector (volts/meter), σ_m is the stress vector (N/m^2), d_{jk}^{c} and d_{im}^{d} are the piezoelectric constants (m/V or C/N), e_{ij}^{σ} is the dielectric permittivity (N/V^2 or F/m), and S_{km}^{E} is the elastic compliance matric (m^2/N). This piezoelectric effect occurs in non-conductive materials and the piezoelectric materials can be separated into two groups: crystals and ceramics.

2.2 PIEZOELECTRIC GENERATORS

For many years, piezoelectric ceramics have been used to convert mechanical vibrations into energy. It has attracted a lot of attention due to its ability to capture surrounding ambient energy and converting it into usable electrical energy and integrated into a system. The research for the generators has been included into buildings, cars, and even the medical field.

Research was trialed in Japan in 2007, where piezoelectric floors were implemented in the East Japan railway stations where electricity was generated from passerby's footsteps. This electricity generated provided power for the automated ticket gates and electronic display systems [36].

Research has been conducted involving implementing piezoelectric generator systems into the Attiki Odos traffic grid. This study took into account where the traffic was heavily loaded on the Greek roads while the major factors consisted of the length of the road being used, the number of vehicles that passed through the area, the kWh of electrical energy, and assessing the electrical energy to the local urban areas [34].

Research in educational buildings such as libraries was conducted at Macquarie University in Sydney, Australia. The study involved strategically placing tiles in high traffic areas in the central hub library. This involved three groups: book borrowers, fixed students, and staff [35].

Piezoelectric ceramics can also be used in the medical field. One journal article presents research suggesting that the PZT can generate enough energy for low power microprocessors and sensors for diagnostic and monitoring applications. These operations are for total knee replacements (TKR) and total hip replacements (THR). The embedded implant sensors have the capability to process measurements, store results, and send the information without harming the body to the surgeon or therapist [28].

2.3 **PIEZOELECTRIC EQUIVALENT CIRCUIT**

A major challenge researcher's face in the field of piezoelectric generators is designing an accurate model for the system. These models range from being a simple single degree of freedom (SDOF) to more complicated models. An equivalent circuit model can capture the number of piezoelectric modes and retains the characteristics of a given circuit. This experiment consisted of a single degree of freedom involving a fixed-free cantilever beam with the given dimensions in Chapter 3 and one piezoelectric ceramic disk. Equation 3 relates the system in Figure 3 to the equation of motion for a SDOF system.

$$m\ddot{x} + d\dot{x} + cx = F + \alpha U$$

$$\frac{1}{C}[Q - \alpha x] + R\left[\dot{Q} - \alpha\dot{x}\right] = U \qquad (3)$$

Where x is the generalized coordinate or tip displacement and m is the modal mass.

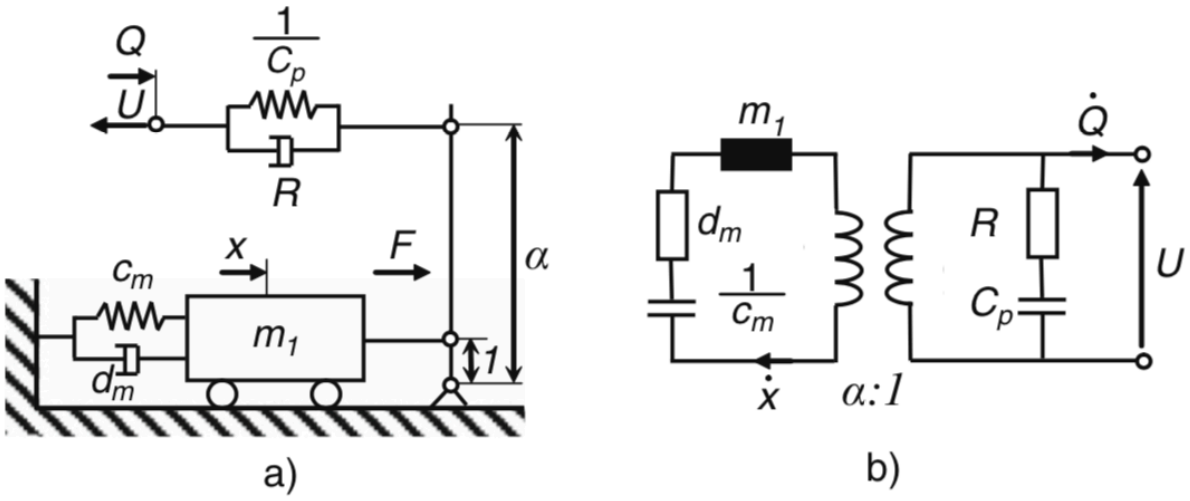

Figure 3: Equivalent circuit model representations, (a) Mechanical and (b) Electrical [33]

2.4 PIEZOELECRTUC CONSTANTS

Since piezoelectric crystals are direction-dependent, it can be said that the ceramics are anisotropic. This means the physical constants (elasticity, permittivity) are tensor quantities and relate to both the direction of the applied stress and electric field, as well as to the directions perpendicular to these. Because of this, the constants have two related quantities. The subscript represents the direction of the two quantities and the superscript index indicates the quantity is kept constant.

The direction of positive polarization is chosen to coincide with the z-axis of a rectangular system of crystallographic axes x, y, and z. The directions of x, y, and z are represented by 1, 2, and 3 respectively while 4, 5, and 6 are the shears about these axes respectively (Figure 4). The constants' subscripts will refer to these.

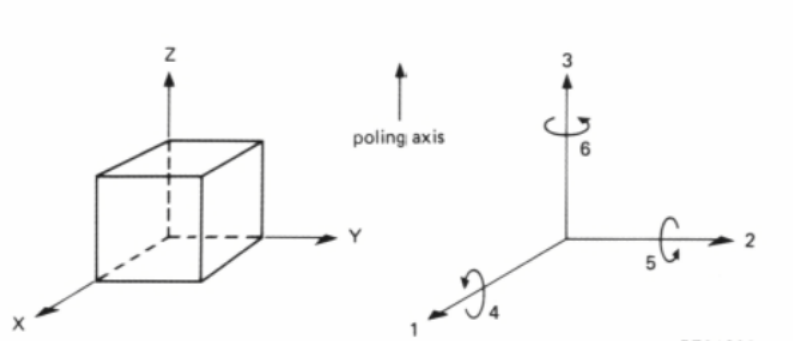

Figure 4: Axes and direction of deformation

2.4.1 PERMITTIVITY (ε)

Permittivity is defined as the dielectric displacement per unit electric field. It is the ability of a substance to store electrical energy in an electric field. The subscripts give the directions of the dielectric displacement and of the electric field, respectfully.

For example:

- ε_{11}^{T} is the permittivity for the dielectric displacement and electric field in direction 1 (x-axis) under constant stress.
- ε_{33}^{S} is the permittivity for the dielectric displacement and electric field in direction 3 (z-axis) under constant strain.

2.4.2 ELASTIC COMPLIANCE (s)

Defined as the strain of an elastic body produced per unit stress. It is the inverse of the modulus of elasticity. The two subscripts refer to the direction of the strain and stress.

For example:

- s_{11}^{E} is the compliance for a stress and accompanying strain in the 1 direction under the circumstances of constant electric field.
- s_{36}^{D} is the compliance for shear stress (6) about the z-axis (3) and accompanying strain in direction 3 under conditions of constant electric displacement.

2.4.3 PIEZOELECTRIC CHARGE CONSTANT (*d*)

The piezoelectric charge constant is the electric polarization generated per unit of mechanical stress applied to a piezoelectric material or is the mechanical strain experienced by a piezoelectric material per unit of electric field applied. The first subscript to d refers to the direction of polarization generated in the material when the electric field (E) is zero or to the applied field strength. The second subscript refers to the direction of applied stress or induced strain. d is an important indicator of a material's suitability for strain-dependent (actuator) applications.

For example:

- $\boldsymbol{d_{33}}$ is the induced polarization per unit applied stress in direction 3. Alternatively, it is the induced strain per unit electric field in direction 3.
- $\boldsymbol{d_{31}}$ is the induced polarization in direction 3 per unit stress applied in direction 1. Alternatively, it is the mechanical strain induced in the material in direction 1 per unit electric field applied in direction 3.
- $\boldsymbol{d_{15}}$ is the induced polarization in direction 1 per unit shear stress applied about direction 2. Alternatively, it is the induced shear strain about direction 2 per unit electric field applied in direction 1.

2.4.4 PIEZOELECTRIC VOLTAGE CONSTANT (*g*)

The piezoelectric voltage constant, g_{ij}, is defined as the electric field generated by a piezoelectric material per unit mechanical stress applied to it. Alternatively, it is the mechanical strain, ε_{ij}, experienced by the material per unit electric displacement applied to it. The first subscript refers to the direction of the electric field generated in the material or to the applied electric displacement and the second refers respectively to the direction of the applied stress or to

the direction of the induced strain. As denoted in equation 3, summation convention does not apply to the repeated indice.

$$g_{ij} = \frac{d_{ij}}{\epsilon_{ii}^{T}} \qquad (3)$$

g is important for assessing a material's suitability for sensing application because the strength of the induced electric field produced by a piezoelectric material in response to an applied physical stress is the product of the value for the applied stress and the value for g.

For example:

- g_{33} is the induced electric field in direction 3 per unit stress applied in direction 3. Alternatively, the induced strain in direction 3 per unit electric displacement applied in direction 3.
- g_{31} is the induced electric field in direction 3 per unit stress applied in direction 1. Alternatively, the induced strain in direction 1 per unit electric displacement applied in direction 3.
- g_{15} is the induced electric field in direction1 per unit shear stress applied about direction 2. Alternatively, the induced shear strain about direction per unit electric displacement applied in direction 1.

2.4.5 COUPLI NG FACTOR (*k*)

The coupling factor is an indicator that shows the effectiveness when a piezoelectric material converts electrical energy into mechanical energy or vice versa. The first subscript denotes the direction along which the electrodes are applied and the second denotes the direction along which the mechanical energy is applied or developed. For frequencies below the resonant frequency of the piezoelectric body, k_{eff} is given by the expression:

$$k_{eff}^2 = \frac{converted\ energy}{input\ energy} \qquad (4)$$

k values quoted in ceramic suppliers' specifications are usually at theoretical maximum values. At low input frequencies, a typical piezoelectric ceramic can convert 30 – 75% of the energy delivered to it in one form into the other form, depending on the formulation of the ceramic and the directions of the forces involved. A high k is usually desirable for efficient energy conversion, but k does not account for dielectric losses or mechanical losses, nor for recovery of unconverted energy.

Since the PZT is a ceramic element, it can dictate unique expressions of k. For the thin, ceramic PZT disk the planar coupling factor (k_p) expresses radial coupling. This is the coupling between an electric field parallel to the direction in which the ceramic element is polarized (direction 3) and mechanical effects that produce radial vibrations, relative to the direction of polarization (direction 1 and direction 2). For a disc whose surface dimensions are large relative to its thickness, the coupling factor (k_t), a unique expression of k_{33}, expresses the coupling between an electric field in direction 3 and mechanical vibrations in the same direction.

2.5 POTENTIAL OF NANOPARTICLES

There has been a growth and impact of nanoscience and nanotechnology in the industry and modern life. Advantages on a nanoscale (1 – 100 nanometers) consist of the properties becoming more advanced and there are significant changes in their physico-chemical properties, such as the chemical, electric, optical, thermal and magnetic characteristics [6]. With this known, nanoparticles can be used for piezoelectric purposes when combined in a field of miniature size. It is important to note the Curie temperature, because at that point the magnetism is lost at the critical temperature.

2.5.1 BARIUM TITANATE ($BaTiO_3$)

Barium Titanate was the first piezoelectric ceramic developed. It has substantially higher coupling factors than any other previously known material. It is also more stable than Rochelle salt, has a wider temperature range of operation, and has an advantage of easy manufacture by ceramic techniques. Table 1 contains the chemical and physical properties of barium titanate.

Table 1: BaTiO3 Properties

Chemical Formula	$BaTiO_3$
Molar Mass	233.192 g/mol
Appearance	White crystals
Odor	Odorless
Density	6.02 g/cm^3, solid
Melting point	1,625 ˚C (2,957 ˚F; 1,898 K)
Water Solubility	Insoluble
Solubility	Slightly soluble in dilute mineral acids; dissolves in concentrated hydrofluoric acid
Band gap	3.2 eV (300 K, single crystal)
Refractive Index (n_D)	No=2.412; n_e=2.360
Crystal Structure	Tetragonal, tP5
Curie Temp	120-130 ˚C

2.5.2 ZINC OXIDE (ZnO)

Zinc oxide (ZnO) on a nanoscale has attracted interest in recent years, as evidenced through numerous publications. This is due to the vast amount of unique properties and potential application of its nanostructures that can be synthesized with great control and precision. Its popularity in ZnO nanowires is much larger than its nanostructures because of the amount of applications involving 0D and 1D nanostructures than that of 2D and 3D nanostructures. Table 2 contains the chemical and physical properties of zinc oxide.

Table 2: ZnO Properties

Properties	
Chemical Formula	ZnO
Molar Mass	81.38 g/mol
Appearance	White solid
Odor	Odorless
Density	5.606 g/cm^3, solid
Melting point	1,975 ˚C (3,587 ˚F; 2,248 K) (decomposes)
Boiling Point	1,975 ˚C (3,587 ˚F; 2,248 K) (decomposes)
Water Solubility	0.0004% (17.8˚C)
Band gap	3.37 eV (direct)
Magnetic susceptibility	-46E-6 cm^3/mol
Refractive Index (n_D)	2.0041
Crystal Structure	Wurtzite

Zinc oxide is tetragonally coordinated which causes the center of the positive charges to overlap with the negative charges. This means that when an external force is applied to the nanostructure it alters the tetrahedron and causes a dipole moment, which results in activating the piezoelectric properties.

2.5.3 STRONTIUM TITANATE ($SrTiO_3$)

Strontium titanate is another nanopowder where there has been interest in the crystals due to it having a high dielectric constant and it has a close relationship with barium titanate. Table 3 contains the chemical and physical properties of strontium titanate.

Table 3: Strontium Titante

Properties	
Chemical Formula	$SrTiO_3$
Molar Mass	183.49 g/mol
Appearance	White, opaque crystals
Density	4.7 g/cm^3
Melting point	2,060 ˚C (3,740 ˚F)
Water Solubility	insoluble
Refractive Index (n_D)	2.394
Crystal Structure	Perovskite

2.5.4 FERROUS NANOPARTICLES

Ferrofluid is a magnetic liquid that is composed of a carriers, surfactants, and magnetic particles. A model can be can be seen in Figure 5. They can be classified based on the choice of carrier, which governs the physical properties, such as organic solvents, hydrocarbons, inorganic solvent, and synthetic esters. Ferrofluid's basic properties, such as retention in a magnetic field, micro-magnetics, levitation of magnetic and non-magnetic objects, are relied upon in engineering applications [7].

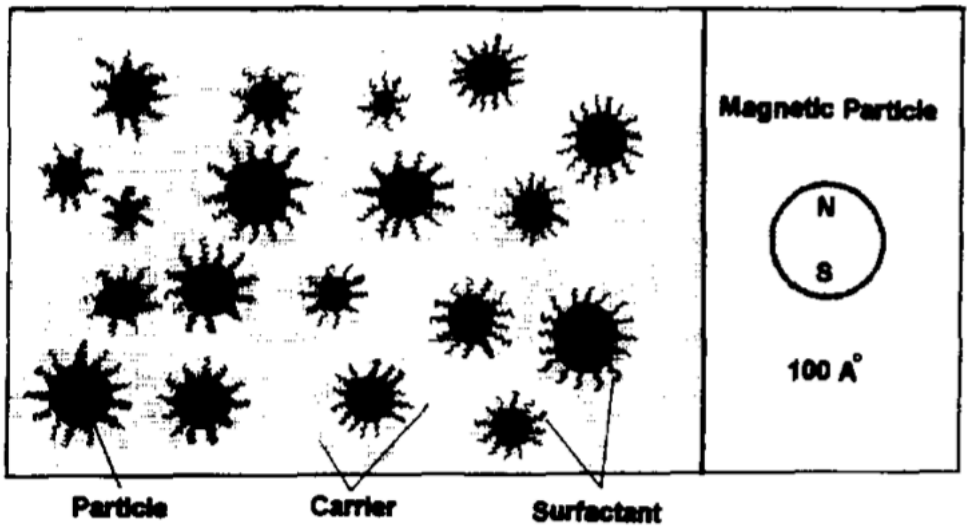

Figure 5: Ferrofluid Components [7]

2.6 SILVER EPOXY/BINDER RESIN

The epoxy consisted of Part A and Part B where the mix ratio had to be 10:1 of the chosen weight. Its primary use was to bond the particles together to create a uniformed coating.

2.7 COATING MIXTURES, SPIN COATING

The coating mixtures contained a mixture composition of nanoparticles and ferrofluid that had been bonded together using a nonconductive epoxy. These compositions become a fluid like material. These surface coatings are applied to the piezoceramic in small quantities and then spin coated. Spin coating provides a way to apply the mixture onto the substrate uniformly. For the average coating, the ceramic is rotationally accelerated to a high speed of 100 rpms for a designated time of 35 seconds. The spinning causes the solution to evenly disperse outward from the center of the disk, leaving a thin film. Depending on the viscosity, the rotational speed and time will be adjusted.

The earliest modeling of spin coating was performed by Emslie *et al* [26]. This was done by solving the equation that describes the flow of a Newtonian liquid on a rotating disk and showed that the film thickness becomes uniformly distributed after the initial distribution of fluid on the disk. There are various mathematical equations as well as a mechanical model [24 – 27].

2.8 DYNAMINC SYSTEM

The dynamic system is forced to vibrate at the same frequency as the excitation, thus subjecting it to a steady-state harmonic excitation. When the frequency of excitation corresponds with the natural frequency of the system, resonance occurs thus allowing the system to oscillate with greater amplitude. Therefore, it is important to calculate the natural frequencies of vibration. The equation of motion for a vibrating beam in flexure is given in equation 5.

$$EI\frac{\partial^4 W}{\partial X^4} + \rho A\frac{\partial^2 W}{\partial t^2} = 0 \qquad (5)$$

Where:

E = Modulus of Elasticity

I = Moment of inertia of beam cross section

W = Displacement of neutral axis

ρ = Beam density

A = Area of beam cross-section

t = Time

From equation 5, using separation of variables approach, the eigenvalue solution gives equation 6.

$$\lambda_n^2 = \sqrt{\frac{\omega_n^2 \rho A}{EI}} \qquad \text{or} \qquad \omega_n = \frac{(\lambda_n L)^2}{L^2}\sqrt{\frac{EI}{\rho A}} \qquad (6)$$

Where:

$\lambda_n =$ Eigen-value of the nth mode.

$\omega_n =$ natural frequency of the nth mode.

For a fixed-free (cantilever beam) boundary condition:

1st mode: $\lambda_1 L = 1.875$

2nd mode: $\lambda_2 L = 4.694$

3rd mode: $\lambda_3 L = 7.855$

Finally, the theoretical natural frequency of the nth mode can be found by dividing the natural frequency of the nth mode by 2*pi. Equation 7 displays this.

$$f_n = \frac{\omega_n}{2\pi} \qquad (7)$$

Equation 6 and equation 7 will be used in chapter 4 to show the theoretical natural frequencies calculated at the first three modes and will be compared to the experimental values.

3 PROCEDURE

The purpose of this experiment is to find a coating mixture that can enhance the power generated from a low-energy producing piezoelectric ceramic. The coating will consist of either barium titanate, strontium titanate, or zinc oxide nanopowder blended together with ferrofluid using binder resin. Many sample combinations were made in order to see how the mixtures varied, which consisted of a given percentage of nanopowder ranging from 0 until loss of fluidity. The samples were applied to the ceramic via spin coating in order to create an even distribution. This chapter will discuss in great details the procedures for preparing the coating, sensor preparations, and the tools and instruments used in conducting the experiment.

3.1 PREPARATION OF THE COATINGS

Three nanopowders were used in the preparation of the coatings. These nanopowders were barium titanate, zinc oxide, and strontium titanate. The mixtures were prepared using different compositions of the nanopowders, ferrofluid, and binder resin. The barium titanate, zinc oxide, and strontium titanate nanoparticles were in powder form and range between 1 to 100 nm. The nanopowder was ordered from TPL, Inc., an American company located in Albuquerque, New Mexico. The amount of epoxy used consisted of either 1% or 2% of the total weight of the coating mixture. The resin was a mixture of silver and epoxy and had a two part mix ratio of 10:1. The binder resin was ordered from a company named Epoxy Technology. Table 5 is an example of different combinations of mixture used. The amount of nanopowder composition used was

increased until it became unstable, losing its fluidity, and cracking after the curing process. At that point, that was the maximum percentage allowed.

Table 4: BaTiO3 Coating Mixture Samples

Barium Titanate ($BaTiO_3$)	Ferrofluid	Epoxy
0%	100%	0%
0%	99%	1%
5%	94%	1%
5%	93%	2%
10%	89%	1%
10%	88%	2%

3.2 SENSOR PREPARATION

Once the nanocoatings were prepared, the next thing to do was apply it onto the piezoelectric disk. The process consisted of spin coating the mixture onto the disk. To do this, a needle was used to place about 0.2 mL of the substance onto the PZT disk. The disk was spun at 100 RPMs for 35 seconds. The machine used to spin coat can be seen in Figure 5. There was a vacuum that hooked up to the machine which created a suction for the disk to be spun without falling off the center plate as well as a tank filled with compressed air. In some cases, the coating would be too thick for the given settings. This would require increasing the RPMs and even the time the disk would be spun for. Another alternative would to spread the coating out on the disk using some kind of brush then spin it to make sure it would be dispersed evenly. The thickness of the coating on the disk was not accounted for.

Figure 6: Spin Coating Machine and Vacuum

After spin coating, the disk was placed in a desiccator chamber, Figure 6, for curing. Limestone was used in the chamber to absorb any moisture that may be present. The PZT would need three days to fully cure and the surface that the PZT rested on needed to be flat. Once the PZT was cured, wires were soldered to the two 50 mm wires on the PZT. This was done to connect the PZT to the circuit board where there was a 1 mega ohm resistor to complete the closed circuit. The size of the plate and element are 27 and 19.7 millimeters, respectively. The PZT is made of brass and the element contains a porous silver electrode.

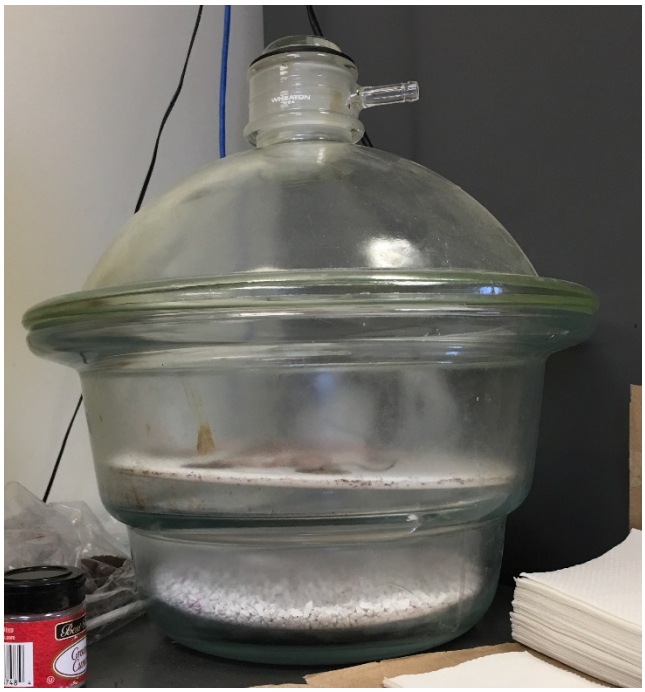

Figure 7: Desiccator Chamber

Figure 7 shows a PZT after the curing process and Figure 8 shows the dimensions in millimeters.

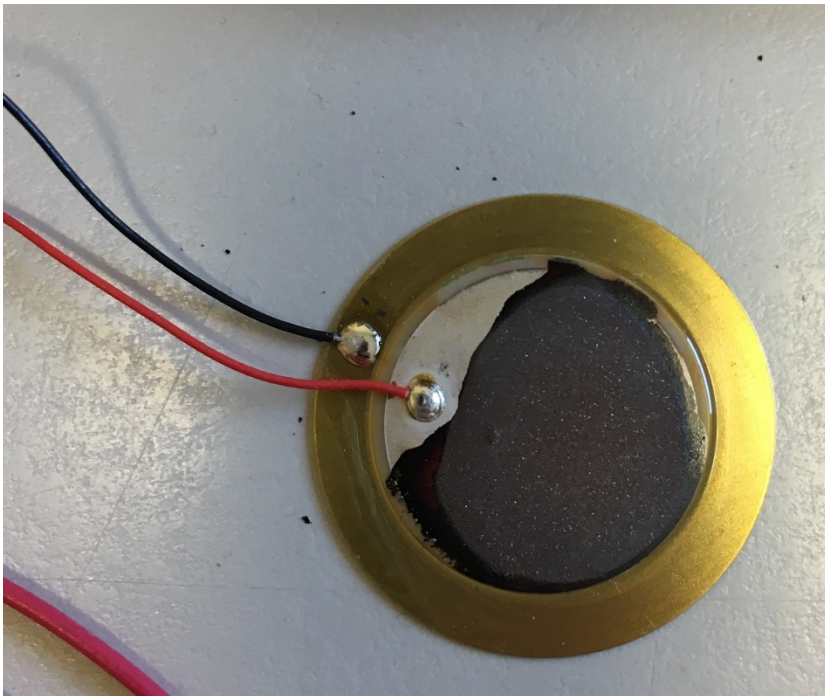

Figure 8: Coated PZT

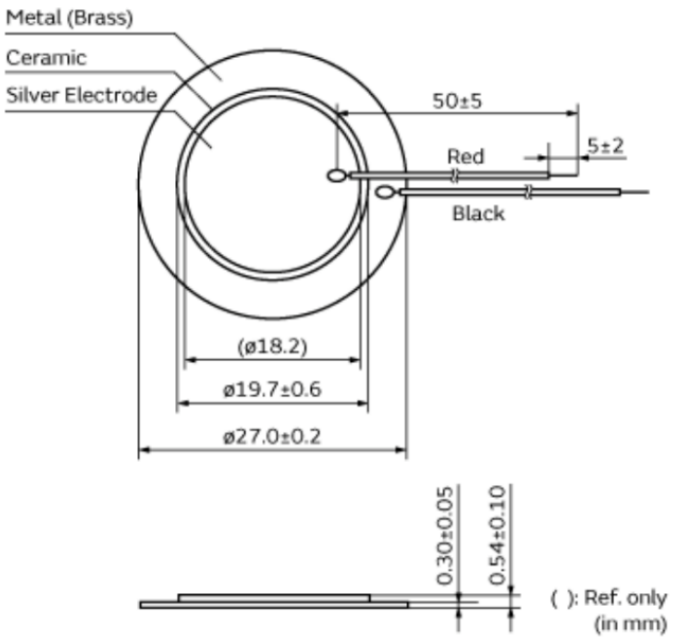

Figure 9: PZT Ceramic Dimensions [37]

Table 6 shows all the specification details about the piezoelectric ceramic. The resonance frequency value is the relative maximum for the response amplitude and can produce large amplitude oscillations while the tolerance is the maximum allowable deviation. Frequency is measured in hertz (Hz). Impedance means including other resisting factors that affect the circuit than just the resistor, and the units are measured in ohms (Ω). The capacitance is the ability to store an electrical charge in the system. Its units are measured in farads (F). The tolerance means the percentage that the system is allowed to deviate away from the values. The plate size refers to the diameter of the metal plate and can be used to calculate the area. The element size refers to the diameter of the ceramic. The plate material is brass. The red and black wires attached to the metal are specified as AWG32 wires and have a length of 50 mm with a tolerance of ±5 millimeters.

Table 5: PZT Specifications [37]

Resonance Frequency	5.0 kHz
Resonant Frequency Tolerance	±0.5 kHz
Resonant Impedance (max.)	300 Ω
Capacitance	20 nF
Tolerance	±30%
Measurement Condition of Capacitance	1 kHz
Shape	Lead
Plate Size	27 mm
Area	5.73E-4 m^2
Element Size	19.7 mm
Plate Material	Brass
Specification of Lead Wire	AWG32
Lead Length	50 mm
Drive Type	External Drive

3.3 THE SETUP

To successfully measure the vibration characteristics of the PZT, many components are needed. These include a function generator, power amplifier, an excitation system with a stainless steel fixed-free beam, a circuit breadboard, and a recorder. Figure 9 shows a general schematic set-up for analyzing the PZT and the experimental set up. Figure 9(a) and 9(b), contain numbers to show what each component looks like and to explain its function.

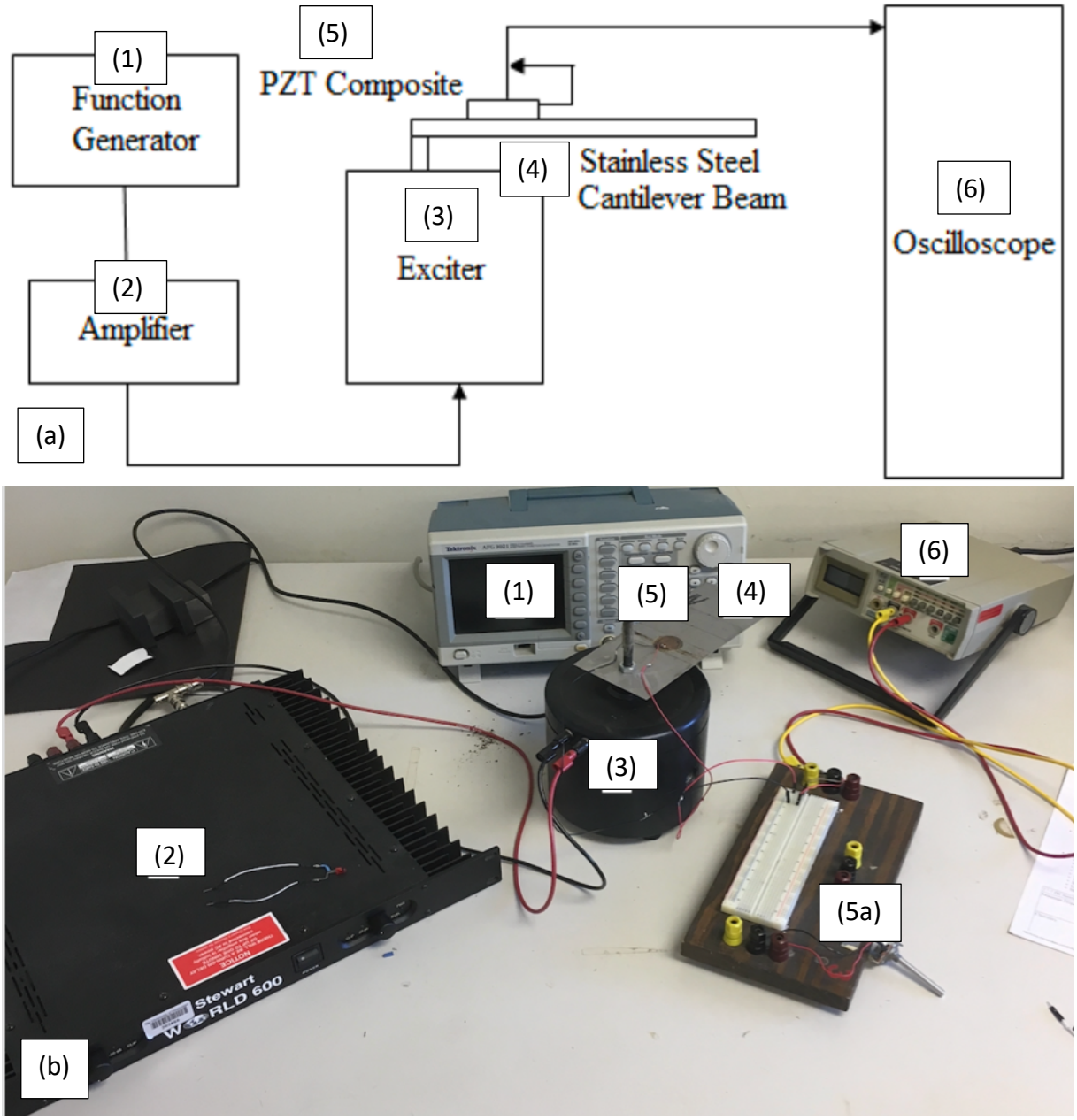

Figure 10: (a) Block Diagram (b) Physical Setup

The function generator (1) was a part of electronic test equipment that controlled the type of generated electrical waveforms in the electromagnetic shaker. The specifications of the function generator were to produce sine outputs and was ran on a continuous mode and the type of the

generator is the Tektronix AFG3021. The function generator transmits the power to the exciter with help from the amplifier (2). The modeled amplifier was a Stewart Audio World 600.

The amplifier applied power to the exciter (3). There are two main types of excitation systems that can be used. One is an impulse hammer and the other is the electromagnetic shaker. The shaker was used because of its ability to control frequency, magnitude, and the type of input force. The type of the modeled shaker used was the Burel & Kjaer Vibration Exciter Type 4809.

Attached on the shaker is a stainless-steel beam (4) that's one sided, and it's fixed-free. The beam is rectangular and its dimensions consist of a length of 199.6 mm, a width of 83.1 mm, and a height of 0.5 mm. For experimental purposes, the length was measured from the hole in the beam to the farther end. There are three points marked on the beam for PZT placement (5). The PZTs were placed onto the steel beam using an adhesive, double sided tape, while the wires from the PZT ran onto a circuit breadboard (5a) and it enclosed a circuit. This way the voltage produced could be measured using an oscilloscope (6). The oscilloscope can measure Direct Current (DC) and Alternating Current (AC). For the experiment, the oscilloscope was set on alternating current. The model of the oscilloscope was a Fluke 8010A Digital Multimeter.

4 RESULTS AND DISCUSSION

Using the setup from the previous chapter, multiple experiments were conducted to observe the effects of the barium titanate, zinc oxide, and strontium titanate nanoparticles on the PZT composite. The source of energy used was mechanical vibration. The results from the experiment are discussed in this chapter.

In order to find the optimum power output, different coating mixtures were created and tested under the same mechanical input vibrations at 1 megaohm resistance. These results show the current generated and power output at the first mode of vibration, while the Appendix will contain the second and third modes. In order to find the modes of vibration, the natural frequencies were needed to be found.

4.1 NATURAL FREQUENCY OF THE CANTILEVER BEAM

In this experiment, it is important to note that the procedure was carried out using a fixed-free cantilever beam. The first three modes of vibration were of interest in order to properly measure the piezoelectric ceramics and record the best possible power output. The beam had the dimensions 0.1736 m x 0.0831 m x 0.0005 m for length (L), width (b), and height (h), respectively. It is important to note that the length of the beam was measured from the hole in the steel to the free end. With the dimensions and other given values, the theoretical natural frequencies were able to be found by recalling Equation 7. Substituting Equation 6 into Equation 7 yields equation 8.

$$f_n = \frac{(\lambda_n L)^2}{2\pi}\sqrt{\frac{EI}{\rho A L^4}} \qquad (8)$$

where:

E = Modulus of Elasticity (204 GPa)

ρ = density of the stainless-steel beam (7810 kg/m^3)

A = cross-sectional area of beam (width (b) x height (h))

L = length of fixed-free beam

I = moment of inertia of the beam cross section and can be calculated using equation 9

$$I = \frac{bh^3}{12} \qquad (9)$$

For the fixed-free (cantilever beam) boundary condition:

First Mode: $\lambda_1 L = 1.875$

Second Mode: $\lambda_2 L = 4.694$

Third Mode: $\lambda_3 L = 7.855$

From equations 8 and 9, the theoretical frequency calculated at the first, second, and third mode were 13.696 Hz, 85.837 Hz, and 240.371 Hz, respectively. These values were relatively close to the natural frequencies, which were 13.6 Hz, 85 Hz, and 232 Hz. Finding the relative percent change with respect towards the theoretical frequencies, the first, second, and third modes were calculated to have percentages of 0.7%, 0.98%, and 3.5%, respectively. Using the natural frequencies, a range was conducted above and below this frequency in order to find the maximum voltage and power output.

4.2 RESULTS OF NONCOATED PZT

Figure 11 shows the power output in microwatts and voltage output (in volts) as dual vertical axes of a noncoated PZT sample. The peak values occur around 13.5 hertz. This data will be compared to the various coatings in order to provide insights as to the nanopowder coatings

either enhancing or diminishing the power output. The maximum power obtained was 1,030.41 microwatts, which occurred at a frequency of 13.4 hertz. With this value, the relative percentage can be found for each mixture, which will tell how well the mixtures compare relative to a noncoated piezoelectric.

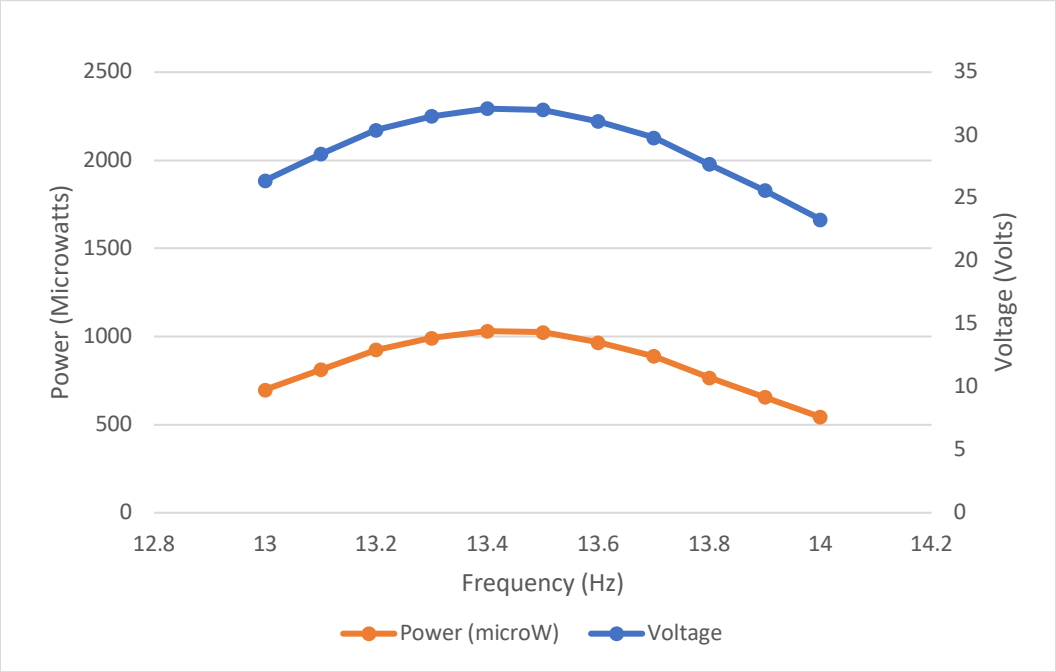

Figure 11: Noncoated Power Output v. Frequency

4.3 RESULTS OF THE BARIUM TITANATE (W/ 1% AND 2% EPOXY) NANOCOATING

4.3.1 IMPACT OF CHANGE IN PERCENTAGE OF EPOXY

Three coatings were prepared with the same nanopowder composition percentage while the ferrofluid and epoxy varied. This was done in order to optimize how much epoxy could be used to bind the nanopowder and ferrofluid to the disk before it became unstable. The nanopowder used was barium titanate which consisted of 10% of the mixture, and the epoxy compositions were

0.5%, 1%, and 2%. The results of each coating can be found in Figure 12. The 10% $BaTiO_3$ + 1% epoxy provided the most power and reached a max peak voltage of 1664.64 microwatts. The second highest coating was 10% $BaTiO_3$ + 0.5% Epoxy. It had a maximum peak voltage of 1474.56 microwatts. Finally, 10% $BaTiO_3$ + 1% epoxy had a maximum peak voltage of 1332.25 microwatts.

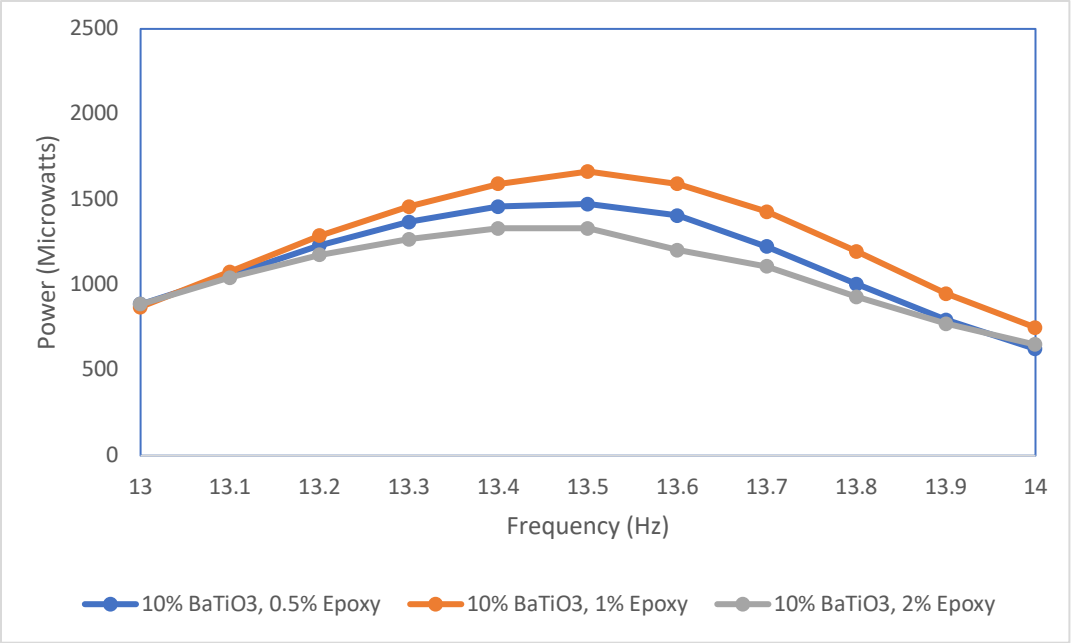

Figure 12: Epoxy Comparison

Even though Figure 12 shows some good results for 10% $BaTiO_3$ + 0.5% epoxy, the experimental procedure showed that it was unstable due to cracking. Therefore, using mixtures containing 0.5% epoxy was not applied throughout the rest of the experimental testing's.

4.3.2 2% EPOXY

This was the first coating mixture applied and testing to the piezoelectric ceramics. From looking at Figure 13, there were eight mixtures made and applied as coatings. The mixture of 10% Barium Titanate, 2% epoxy, and 88% ferrofluid generated the highest power output around the

frequency of 13.5 hertz as well as generated power output of 1,332.25 microwatts. The mixture that performed the poorest contained 30% barium titanate, 2% epoxy, and 68% ferrofluid. A possible reason to this is the adhesive (double-sided tape) did not work as efficiently. These results were tested at the first mode. The results from the second and third modes can be seen in the Appendices.

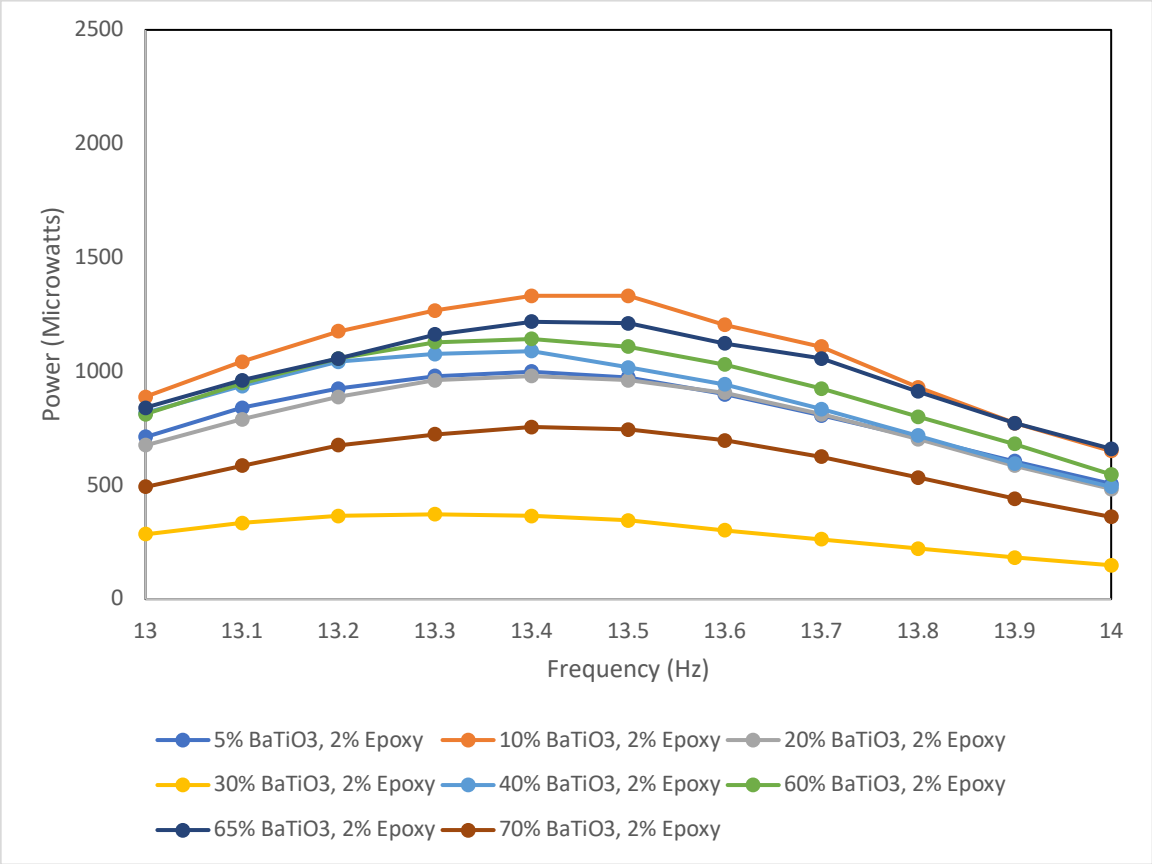

Figure 13: BaTiO3 w/2% Epoxy v. Frequency

Table 6 shows the peak power output of each coating from Figure 13.

Table 6: Barium Titanate + 2% Epoxy

Coating	Max Power (Microwatts)
5% BaTiO3, 2% Epoxy	998.56
10% BaTiO3, 2% Epoxy	1332.25
20% BaTiO3, 2% Epoxy	979.69
30% BaTiO3, 2% Epoxy	372.49
40% BaTiO3, 2% Epoxy	1089
60% BaTiO3, 2% Epoxy	1142.44
65% BaTiO3, 2% Epoxy	1218.01
70% BaTiO3, 2% Epoxy	756.25

4.3.3 1% EPOXY

This test was ran the same as the previous mixture with the exception that 1% epoxy was used instead of 2%. This was to determine how the coatings reacted, whether it'd make the samples unstable or it reacted significantly better. As it can be seen in Figure 14, the mixture of 20% barium titanate, 2% epoxy, and 78% ferrofluid had the greatest power output of 1,892.25 microwatts at a frequency of 13.6 hertz. When compared to the highest power output from the barium titanate sample with 2% epoxy, it has a relative percent of 142%. The mixture of 70% barium titanate, 1% epoxy, 29% performed the worst. This is because the coating was unstable and when it was being vibrated, the coating broke off into flakes. Also, the adhesive of the double-sided tape couldn't have been as strong and durable.

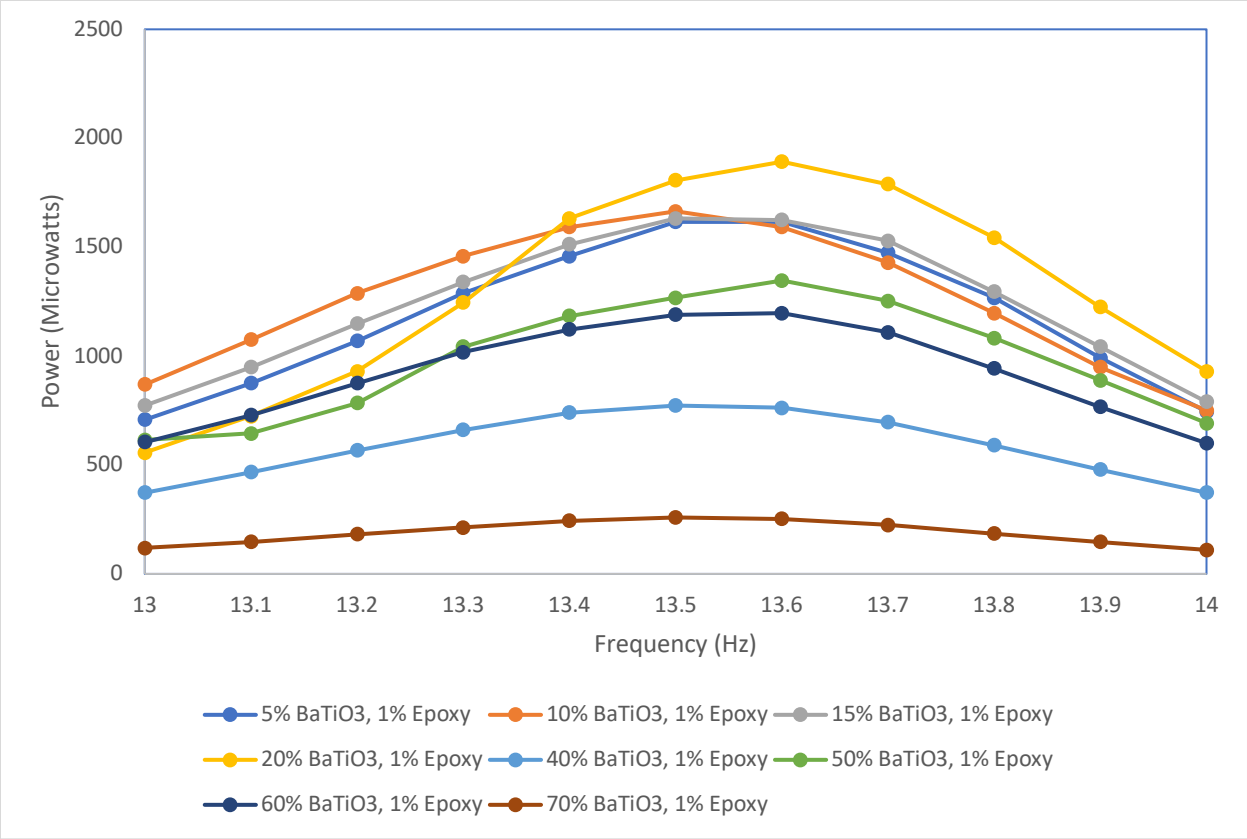

Figure 14: BaTiO3 w/1% Epoxy v. Frequency

Table 7 shows the peak power output of each coating from Figure 14.

Table 7: Barium Titanate + 1% Epoxy

Coating	Peak Power (Microwatts)
5% BaTiO3, 1% Epoxy	1616.04
10% BaTiO3, 1% Epoxy	1664.64
15% BaTiO3, 1% Epoxy	1632.16
20% BaTiO3, 1% Epoxy	1892.25
40% BaTiO3, 1% Epoxy	772.84
50% BaTiO3, 1% Epoxy	1346.89
60% BaTiO3, 1% Epoxy	1197.16
70% BaTiO3, 1% Epoxy	259.21

4.3.4 EPOXY V. NONCOATED

The following graphs (Fig. 15 – Fig. 20) are comparing the power output of the coating mixture of barium titanate with the designated epoxy combination to the noncoated sample. These were ran at the first mode from the frequency range of 13 to 14 hertz.

Figure 15 shows the power outputs of the compositions of 5% barium titanate with 1% and 2% epoxy as well as the noncoated PZT. The 5% composition with 1% epoxy outperformed both the noncoated and the 5% composition with 2% epoxy. At the peak power, the 1% epoxy's power output performed 56% (efficiency value of 1.56) better than the noncoated while the 2% epoxy had a 3% reduction (0.97 efficiency value) of power output than the noncoated.

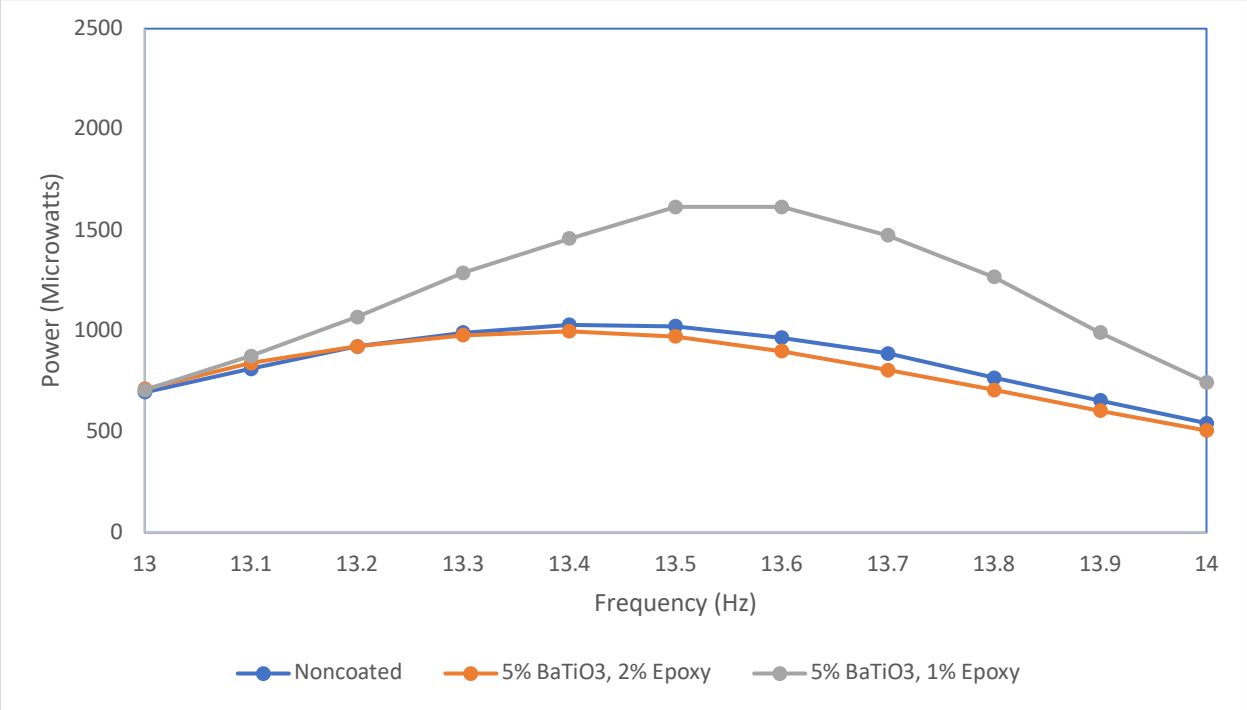

Figure 15: 5% Barium Titanate v. Noncoated PZT

Figure 16 shows the power outputs of the compositions of 10% barium titanate with 1% and 2% epoxy as well as the noncoated PZT. The 10% composition with 1% epoxy outperformed both the noncoated and the 5% composition with 2% epoxy. At the peak power, the 1% epoxy's

power output performed 62% (efficiency value of 1.62) better than the noncoated while the 2% epoxy's power output performed 29% (1.29 efficiency value) batter than the noncoated.

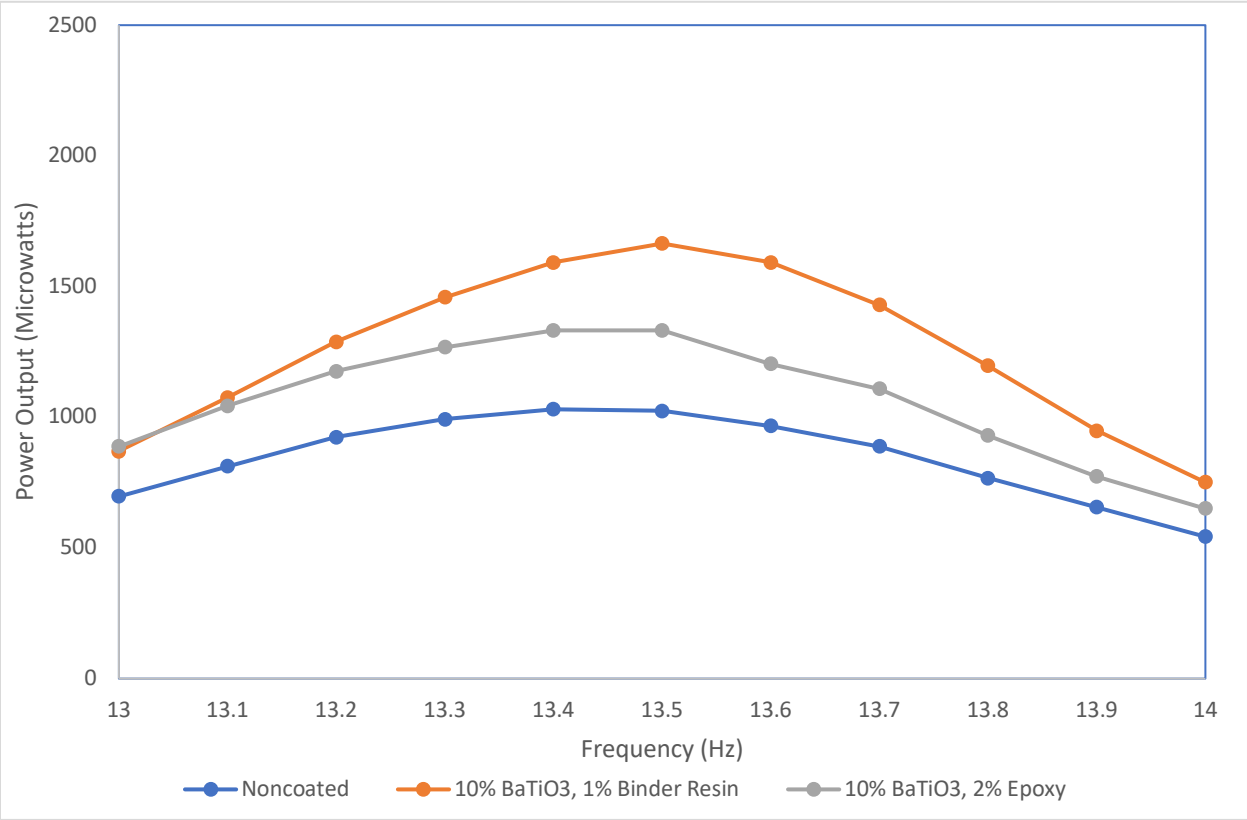

Figure 16: 10% Barium Titanate v. Noncoated PZT

Figure 17 shows the power outputs of the compositions of 20% barium titanate with 1% and 2% epoxy as well as the noncoated PZT. The 20% composition with 1% epoxy outperformed both the noncoated and the 20% composition with 2% epoxy. At the peak power, the 1% epoxy's power output performed 84% (efficiency value of 1.84) better than the noncoated while the 2% epoxy's power output had a reduction of 5% (0.95 efficiency value) of the noncoated.

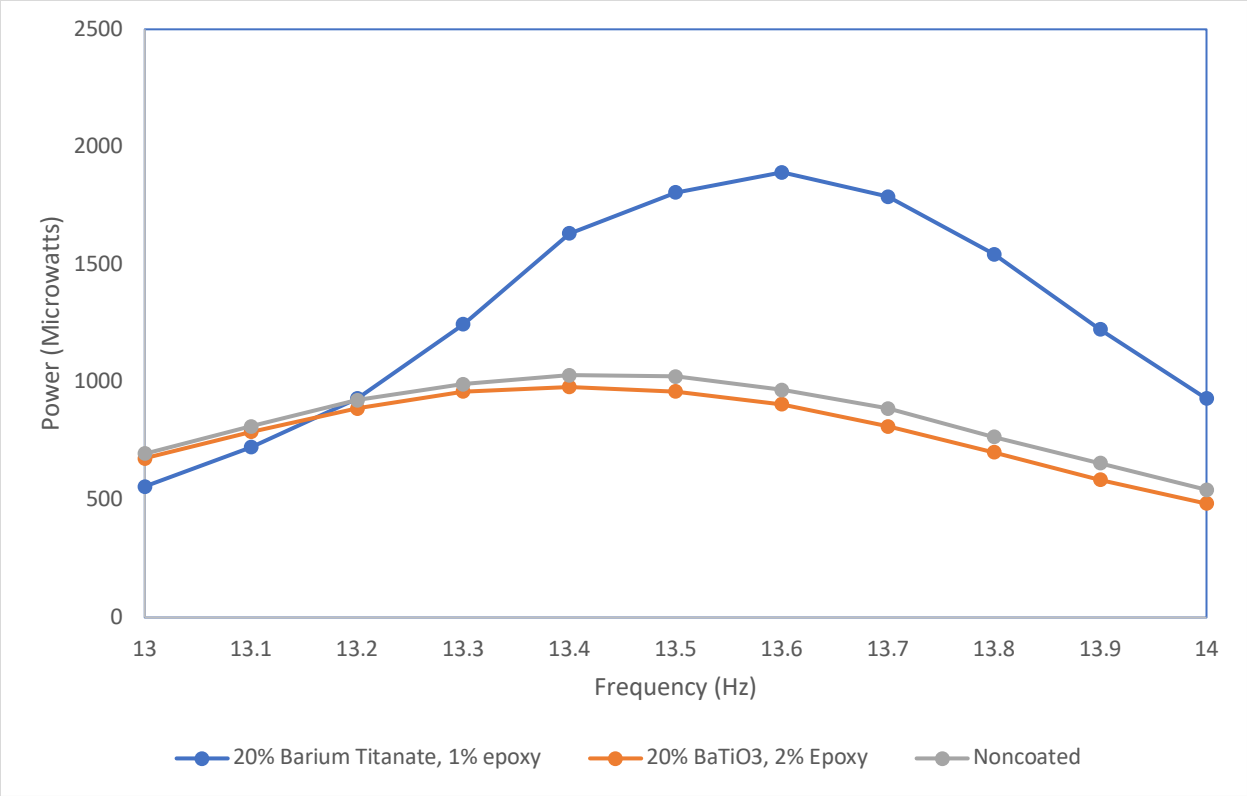

Figure 17: 20% Barium Titanate v. Noncoated PZT

Figure 18 shows the power outputs of the compositions of 40% barium titanate with 1% and 2% epoxy as well as the noncoated PZT. The 40% composition with 2% epoxy outperformed both the noncoated and the 40% composition with 1% epoxy. At the peak power, the 1% epoxy's power output had a reduction of 25% (efficiency value of 0.75) power when compared to the noncoated, while the 2% epoxy's power output performed 6% (1.06 efficiency value) better than the noncoated.

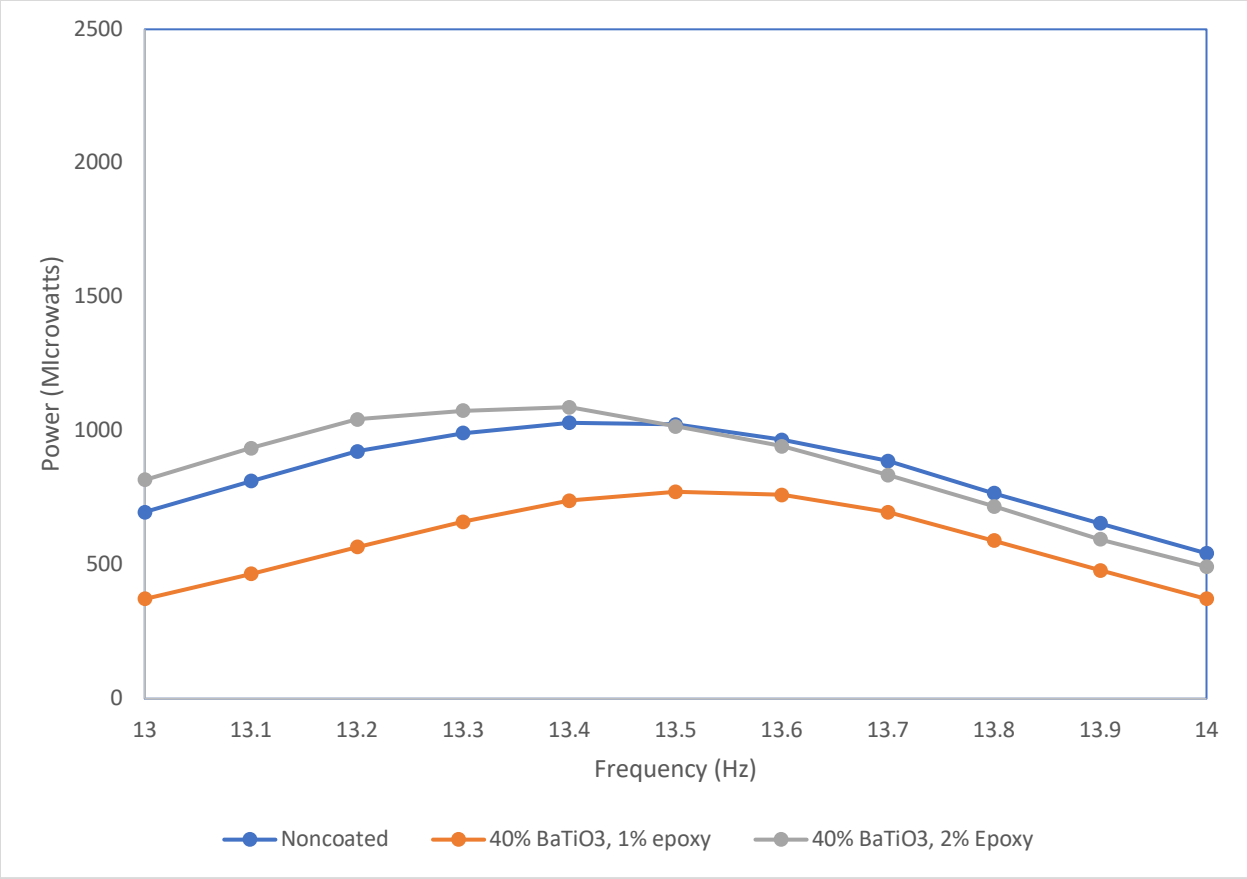

Figure 18: 40% Barium Titanate v. Noncoated PZT

Figure 19 shows the power outputs of the compositions of 60% barium titanate with 1% and 2% epoxy as well as the noncoated PZT. The 60% composition with 1% epoxy outperformed both the noncoated and the 60% composition with 2% epoxy. At the peak power, the 1% epoxy's power output performed 16% (efficiency value of 1.16) better than the noncoated while the 2% epoxy's power output performed 11% (1.11 efficiency value) of the noncoated.

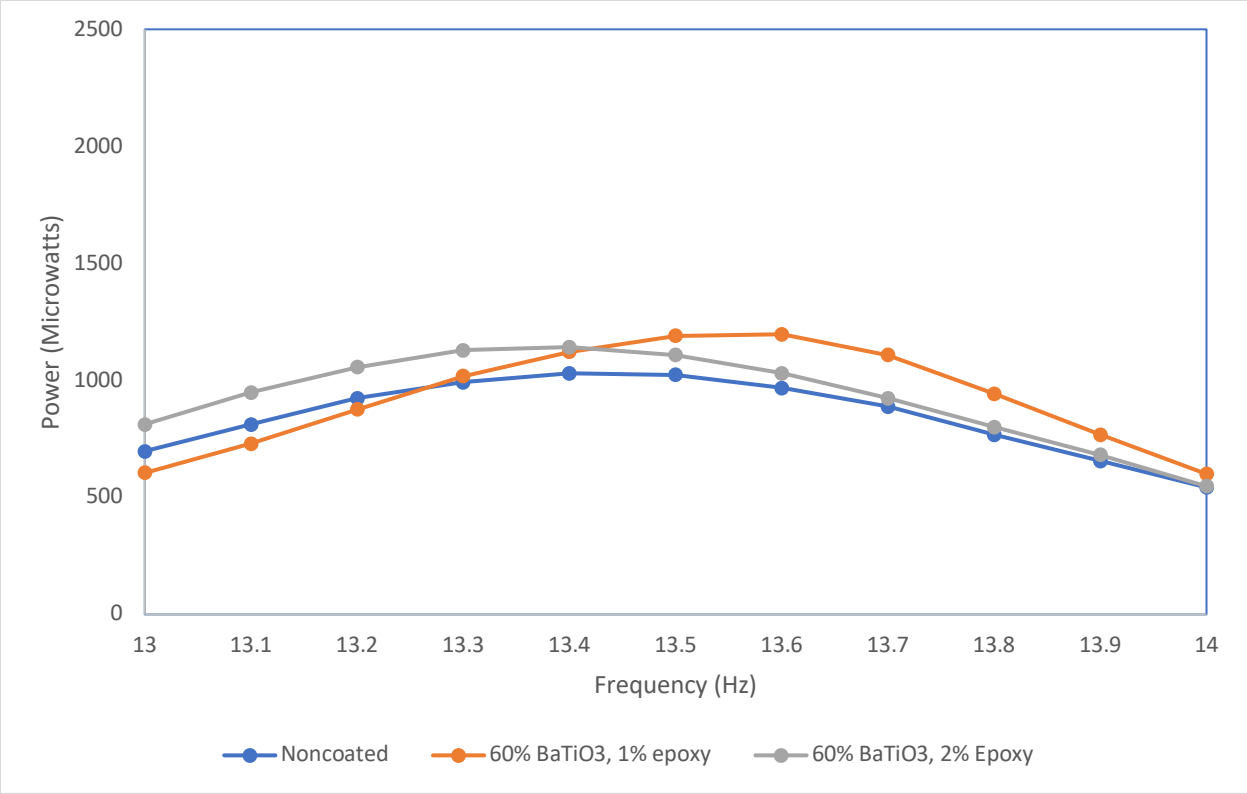

Figure 19: 60% Barium Titanate v. Noncoated PZT

Figure 20 shows the power outputs of the compositions of 70% barium titanate with 1% and 2% epoxy as well as the noncoated PZT. At the peak power, the composition of 70% barium titanate with 1% epoxy's power output had a reduction of 75% (efficiency value of 0.25) than the noncoated power and the composition of 70% barium titanate with 2% epoxy's power output had a reduction of 27% (0.73 efficiency value) of the noncoated power. These values could be due to the fact that the barium titanate coating became very thick and had a high viscosity level. This would've made it harder for the material to disperse uniformly during spin coating.

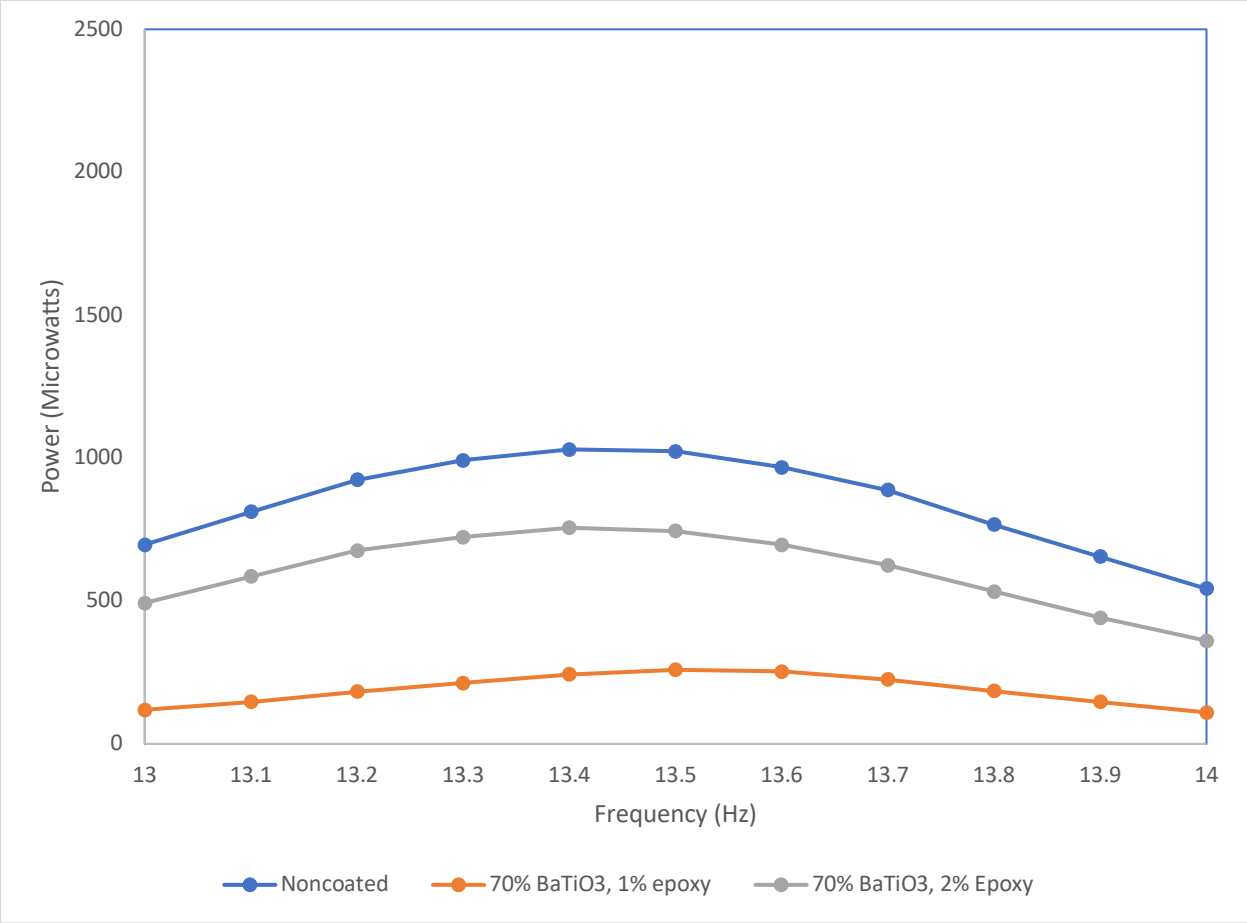

Figure 20: 70% Barium Titanate v. Noncoated PZT

4.4 RESULTS OF ZINC OXIDE (W/ 1% + 2% EPOXY) NANOCOATING

4.4.1 1% EPOXY

Sharma [39] had used many mixtures of zinc oxide, ferrofluid, and epoxy. In the case of using a single composite, he obtained a maximum power output of 44.53 microwatts at 90 hertz for a coating composition of 40% zinc, 0.1% epoxy, and 59.9% ferrofluid. By looking at his findings, there was no recordings around the theoretical natural frequencies.

By looking at Figure 21, the highest power output is produced by the mixture composition of 5% zinc oxide, 1% epoxy, and 94% ferrofluid. This occurred at 13.6 hertz with a power output of 2,070.25 microwatts. This has a relative change of 201%. The mixture containing 40% zinc

oxide, 1% epoxy, and 59% performed the least out of the mixtures, but still out performed the noncoated piezoelectric ceramic. It's power output was 1303.21 microwatts and had a relative change of 126%. Overall, any combination of zinc oxide with 1% epoxy appears to contain the best results for low vibrations when compared to a noncoated piezoelectric disk.

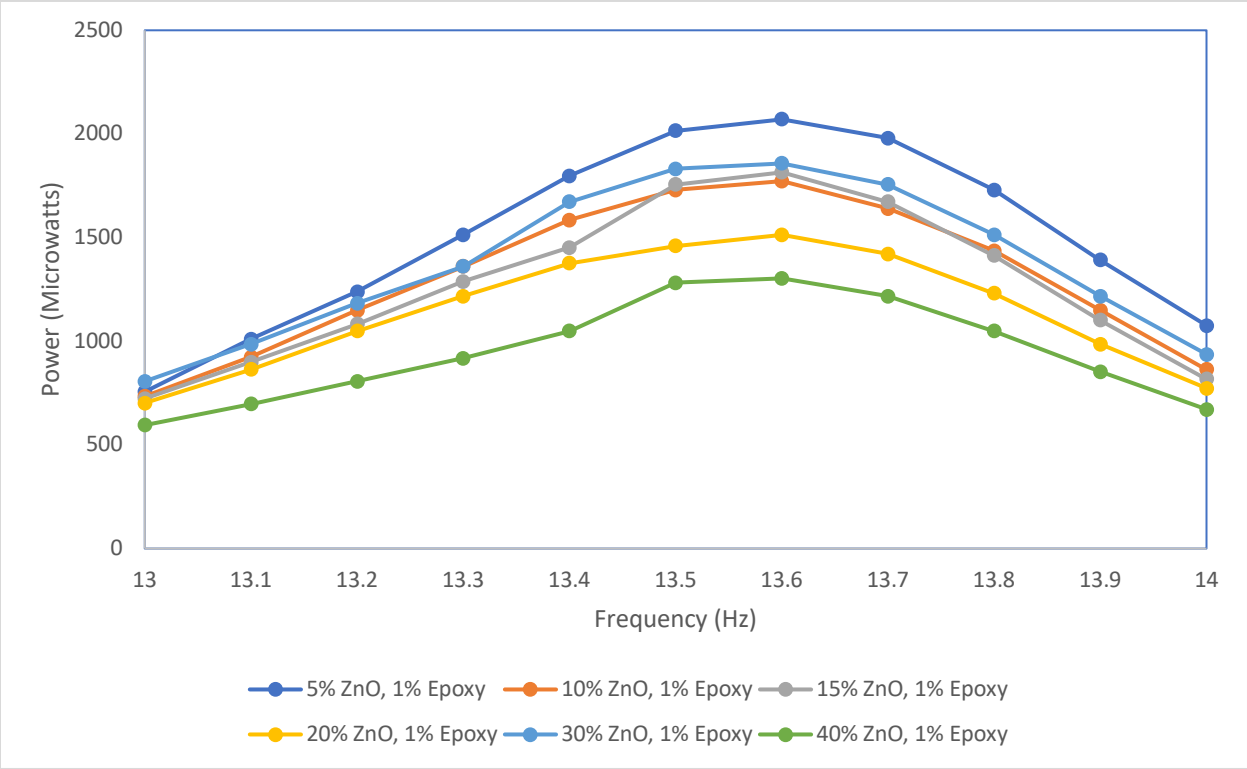

Figure 21: ZnO w/1% Epoxy v. Frequency

Table 8 shows the peak power output of each coating from Figure 21.

Table 8: Zinc Oxide + 1% Epoxy

Coating	Peak Power (Microwatts)
5% ZnO, 1% Epoxy	2070.25
10% ZnO, 1% Epoxy	1772.41
15% ZnO, 1% Epoxy	1814.76
20% ZnO, 1% Epoxy	1513.21
30% ZnO, 1% Epoxy	1857.61
40% ZnO, 1% Epoxy	1303.21

4.4.2 2% EPOXY

From looking at Figure 22, 5% zinc oxide, 2% epoxy, 93% ferrofluid mixture composition has the greatest power output of 2,171.56 microwatts at a frequency of 13.6 hertz. This has a relative change of 211%. When this sample is compared to the zinc oxide sample with 1% epoxy, it has a relative change of 5%. It can also be seen that at 13.6 hertz, each zinc oxide sample reaches its peak power value.

At 13.4 hertz, the composition of 30% ZnO, 2% Epoxy, 68% Ferrofluid takes a noticeable dive before increasing significantly. The reason for this being

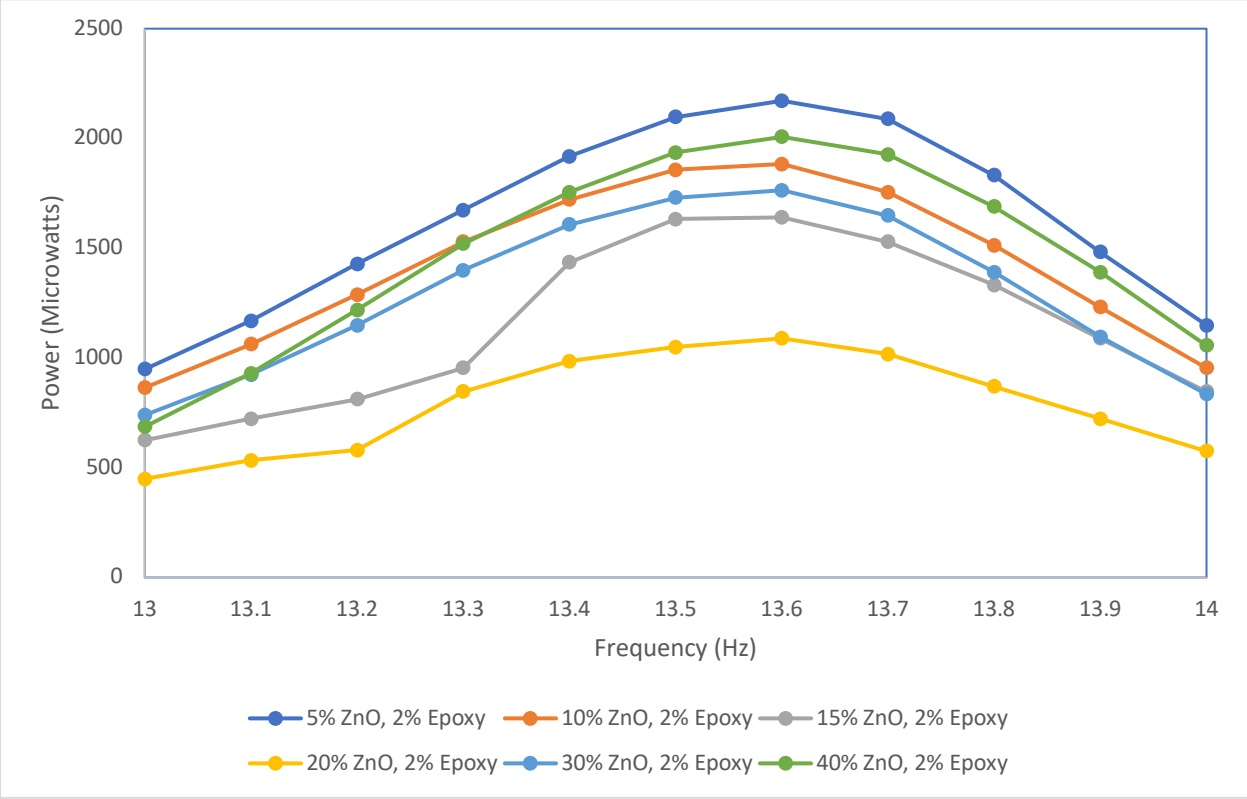

Figure 22: ZnO w/2% Epoxy v. Frequency

Table 9 shows the peak power output of each coating from Figure 22.

Table 9: Zinc Oxide + 2% Epoxy

Coating	Peak Power (Microwatts)
5% ZnO, 2% Epoxy	2171.56
10% ZnO, 2% Epoxy	1883.56
15% ZnO, 2% Epoxy	1640.25
20% ZnO, 2% Epoxy	1089
30% ZnO, 2% Epoxy	1764
40% ZnO, 2% Epoxy	2007.04

4.4.3 EPOXY V. NONCOATED PZT

The following graphs (Fig. 23 – Fig. 28) are comparing the power output of the coating mixture of zinc oxide with the designated epoxy combination to the noncoated sample. These were ran at the first mode from the frequency range of 13 to 14 hertz.

Figure 23 shows the power outputs of the compositions of 5% zinc oxide with 1% and 2% epoxy as well as the noncoated PZT. At the peak power, the composition of 5% zinc oxide with 1% epoxy's power output performed 101% (efficiency value of 2.01) better than the noncoated while the 2% epoxy's power output performed 111% (2.11 efficiency value) better than the noncoated.

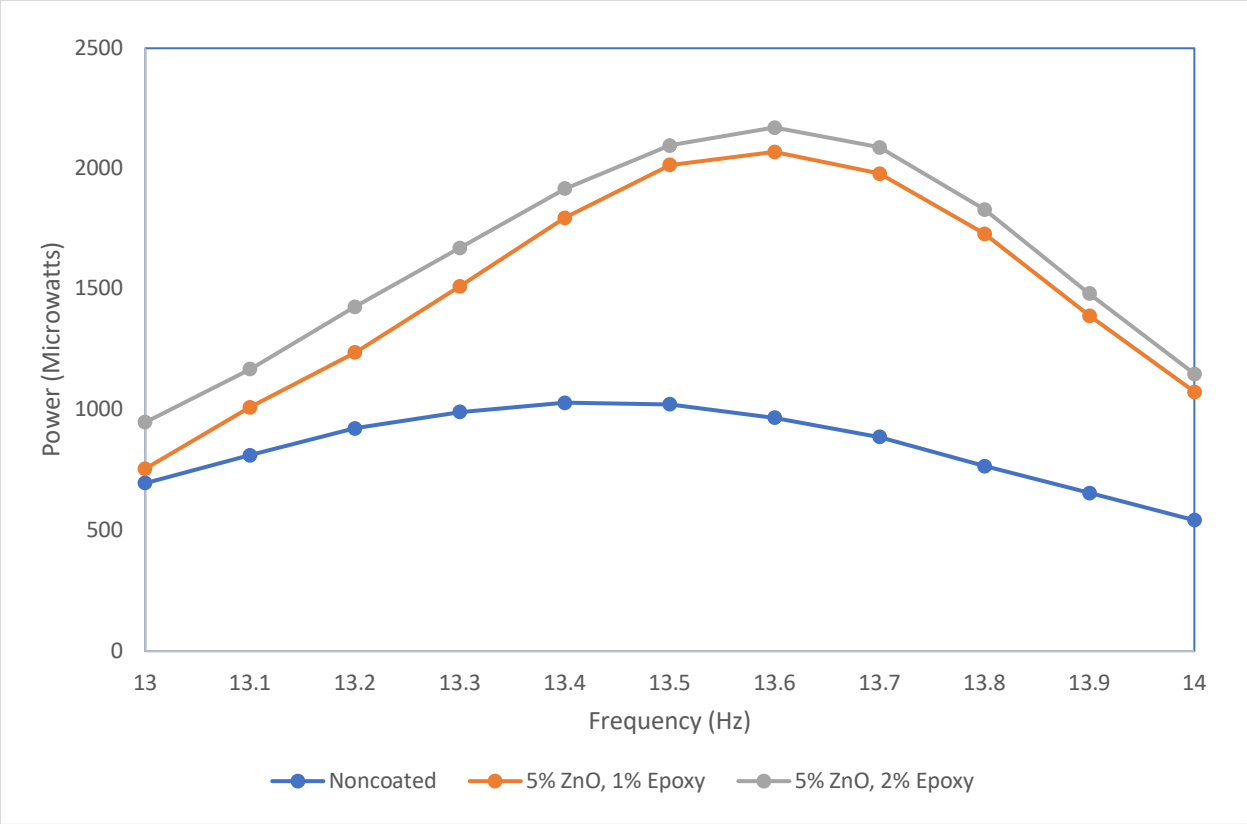

Figure 23: 5% Zinc Oxide v. Noncoated PZT

Figure 24 shows the power outputs of the compositions of 10% zinc oxide with 1% and 2% epoxy as well as the noncoated PZT. At the peak power, the composition of 10% zinc oxide with 1% epoxy's power output performed 72% (efficiency value of 1.72) better than the noncoated while the 2% epoxy's power output performed 83% (1.83 efficiency value) better than the noncoated.

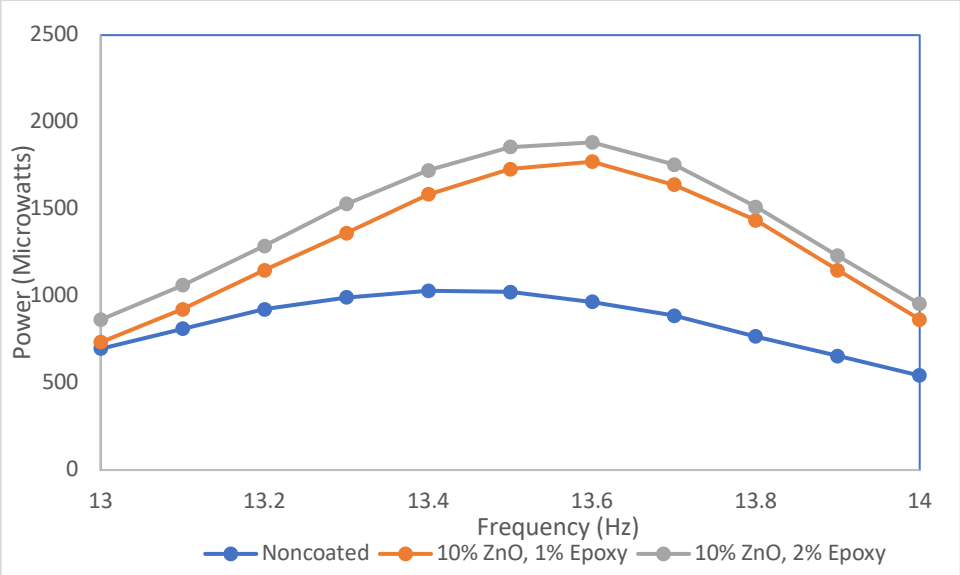

Figure 24: 10% Zinc Oxide v. Noncoated

Figure 25 shows the power outputs of the compositions of 15% zinc oxide with 1% and 2% epoxy as well as the noncoated PZT. At the peak power, the composition of 15% zinc oxide with 1% epoxy's power output performed 76% (efficiency value of 1.76) better than the noncoated while the 2% epoxy's power output performed 59% (1.59 efficiency value) better than the noncoated.

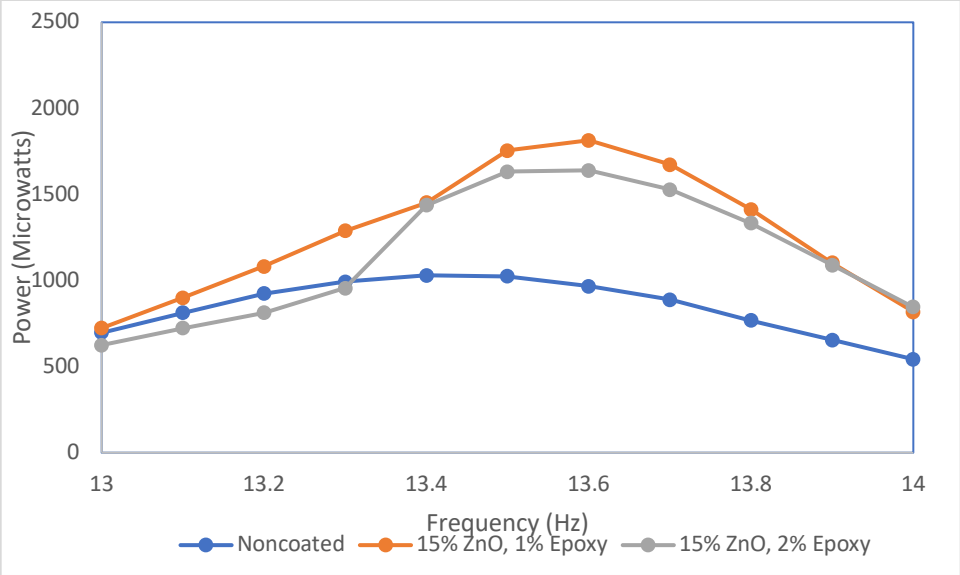

Figure 25: 15% Zinc Oxide v. Noncoated PZT

Figure 26 shows the power outputs of the compositions of 20% zinc oxide with 1% and 2% epoxy as well as the noncoated PZT. At the peak power, the composition of 20% zinc oxide with 1% epoxy's power output performed 47% (efficiency value of 1.47) better than the noncoated while the 2% epoxy's power output performed 6% (1.06 efficiency value) better than the noncoated.

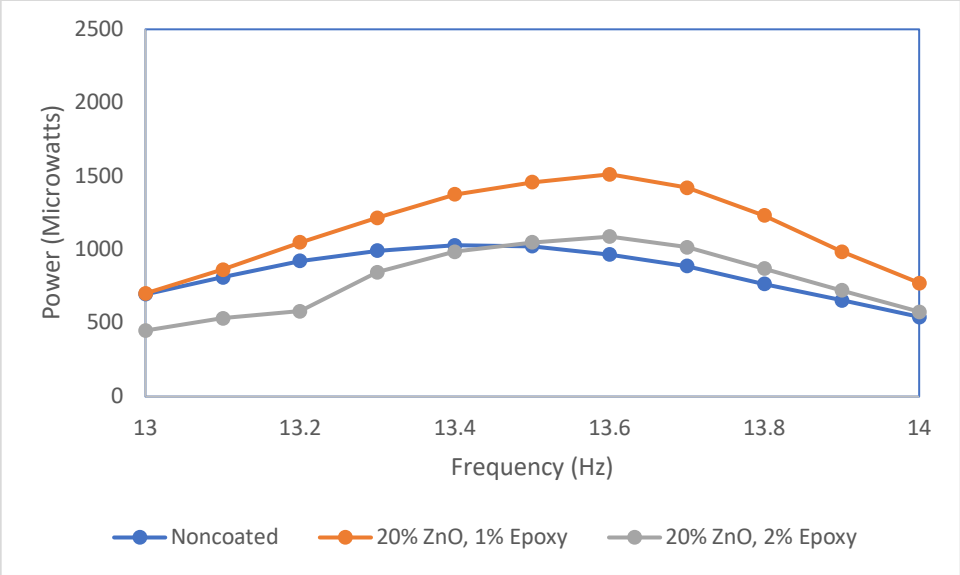

Figure 26: 20% Zinc Oxide v. Noncoated PZT

Figure 27 shows the power outputs of the compositions of 30% zinc oxide with 1% and 2% epoxy as well as the noncoated PZT. At the peak power, the composition of 30% zinc oxide with 1% epoxy's power output performed 80% (efficiency value of 1.80) better than the noncoated while the 2% epoxy's power output performed 71% (1.71 efficiency value) better than the noncoated.

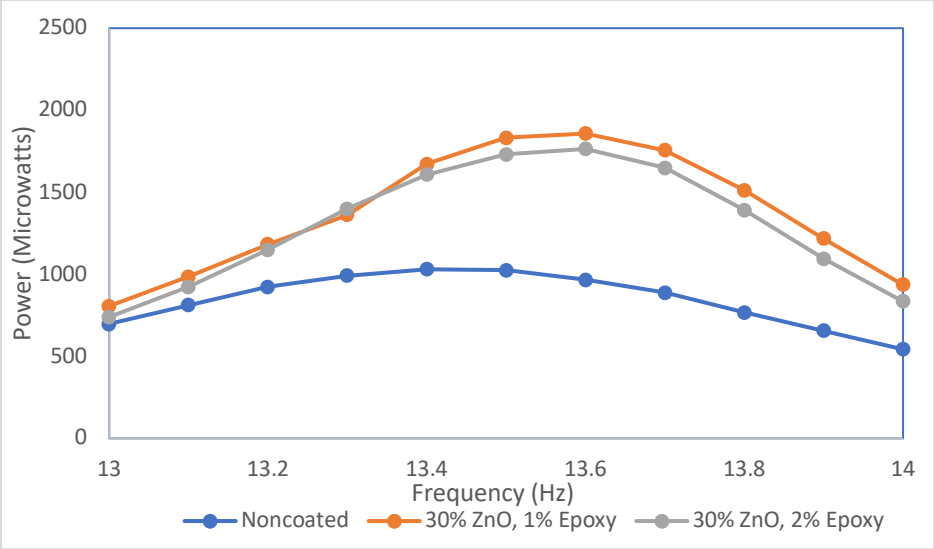

Figure 27: 30% Zinc Oxide v. Noncoated PZT

Figure 28 shows the power outputs of the compositions of 40% zinc oxide with 1% and 2% epoxy as well as the noncoated PZT. At the peak power, the composition of 40% zinc oxide with 1% epoxy's power output performed 26% (efficiency value of 1.26) better than the noncoated while the 2% epoxy's power output performed 95% (1.95 efficiency value) better than the noncoated.

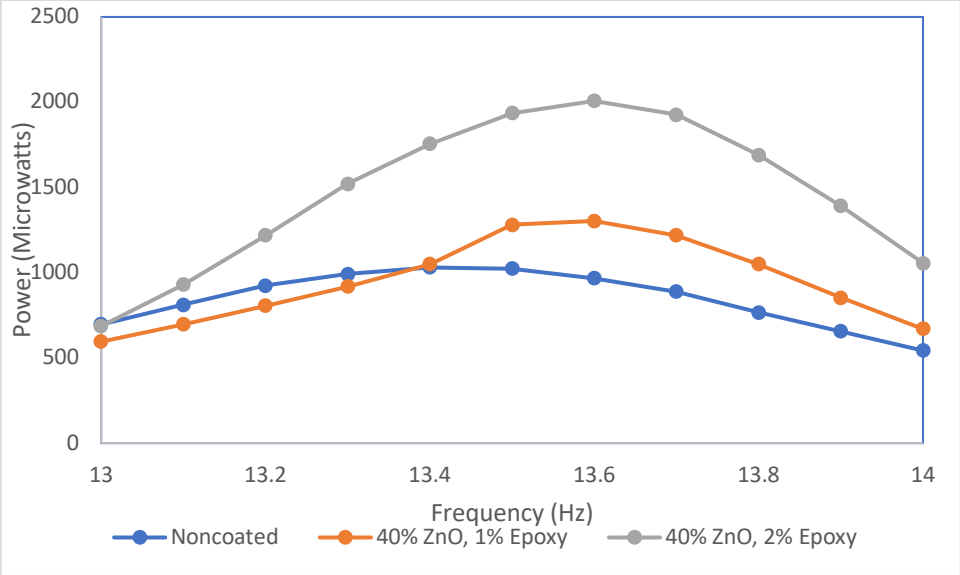

Figure 28: 40% Zinc Oxide v. Noncoated PZT

4.5 EFFECT OF STRONTIUM TITANATE (W/ 1% +2% EPOXY)

4.5.1 1% EPOXY

From Figure 29, the composition of 5% strontium titanate, 1% epoxy, 94% ferrofluid had the greatest power output of 1814.76 microwatts at 13.6 hertz. This had a relative change of 176%. 40% strontium titanate, 1% epoxy, 59% ferrofluid was close with a power value of 1772.41 microwatts at 13.6 hertz, followed by 60% strontium titanate, 1% epoxy, 39% ferrofluid with a power output of 1705.69 microwatts.

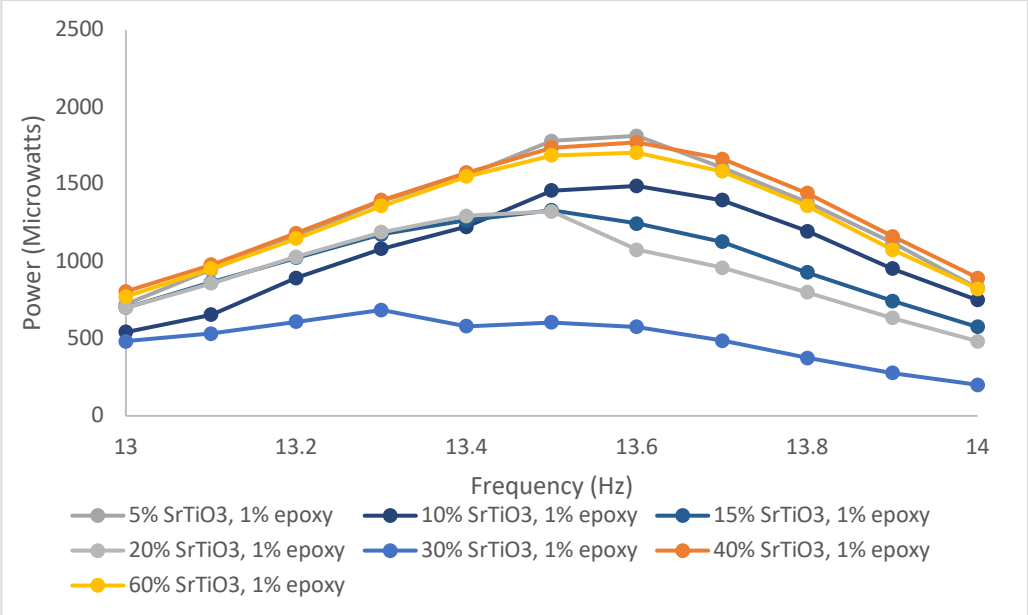

Figure 29: SrTiO3 w/1% Epoxy v. Frequency

Table 10 shows the peak power output of each coating from Figure 29.

Table 10: Strontium Titanate + 1% Epoxy

Coating	Peak Power (Microwatts)
5% SrTiO3, 1% Epoxy	1814.76
10% SrTiO3, 1% Epoxy	1489.96
15% SrTiO3, 1% Epoxy	1332.25
20% SrTiO3, 1% Epoxy	1324.96
30% SrTiO3, 1% Epoxy	686.44
40% SrTiO3, 1% Epoxy	1772.41
60% SrTiO3, 1% Epoxy	1705.69

4.5.2 2% EPOXY

From Figure 30, the composition of 20% strontium titanate, 1% epoxy, 79% ferrofluid had the greatest power output of 2125.21 microwatts at 13.6 hertz. This had a relative change of 206.25%. 30% strontium titanate, 1% epoxy, 69% ferrofluid was close with a power value of 1624.09 microwatts at 13.6 hertz, followed by 5% strontium titanate, 1% epoxy, 94% ferrofluid with a power output of 1576.09 microwatts.

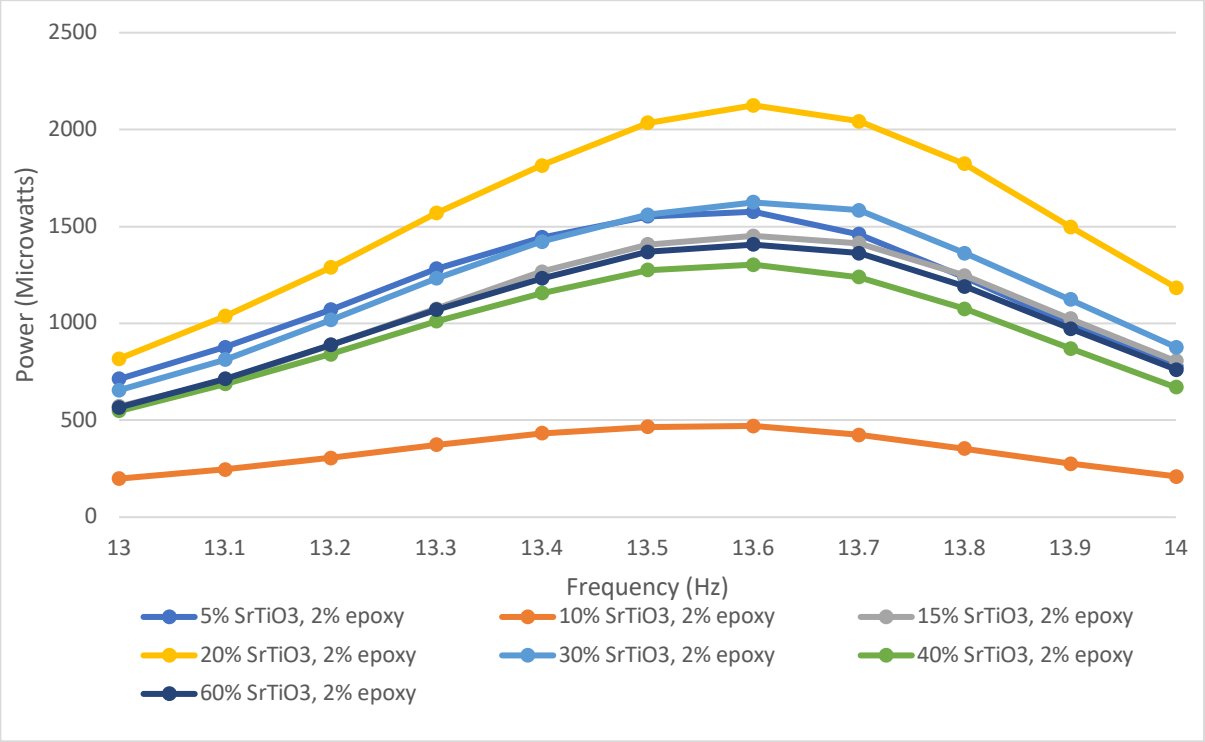

Figure 30: SrTiO3 w/2% Epoxy v. Frequency

Table 11 shows the peak power output of each coating from Figure 30.

Table 11: Strontium Titanate + 2% Epoxy

Coating	Peak Power (Microwatts)
5% SrTiO3, 2% Epoxy	1576.09
10% SrTiO3, 2% Epoxy	470.89
15% SrTiO3, 2% Epoxy	1451.61
20% SrTiO3, 2% Epoxy	2125.21
30% SrTiO3, 2% Epoxy	1624.09
40% SrTiO3, 2% Epoxy	1303.21
60% SrTiO3, 2% Epoxy	1406.25

4.5.3 EPOXY V. NONCOATED PZT

Figure 31 shows the power outputs of the composition of 5% strontium titanate with 1% epoxy and 2% epoxy as well asthe noncoated PZT. At the peak power, the composition of 5% strontium titanate with 1% epoxy's power output performed 76% (efficiency value of 1.76) better than the noncoated. The compositition of 5% strontium titanate with 2% epoxy enhanced the traditional PZT by 53% (efficiency value of 1.53).

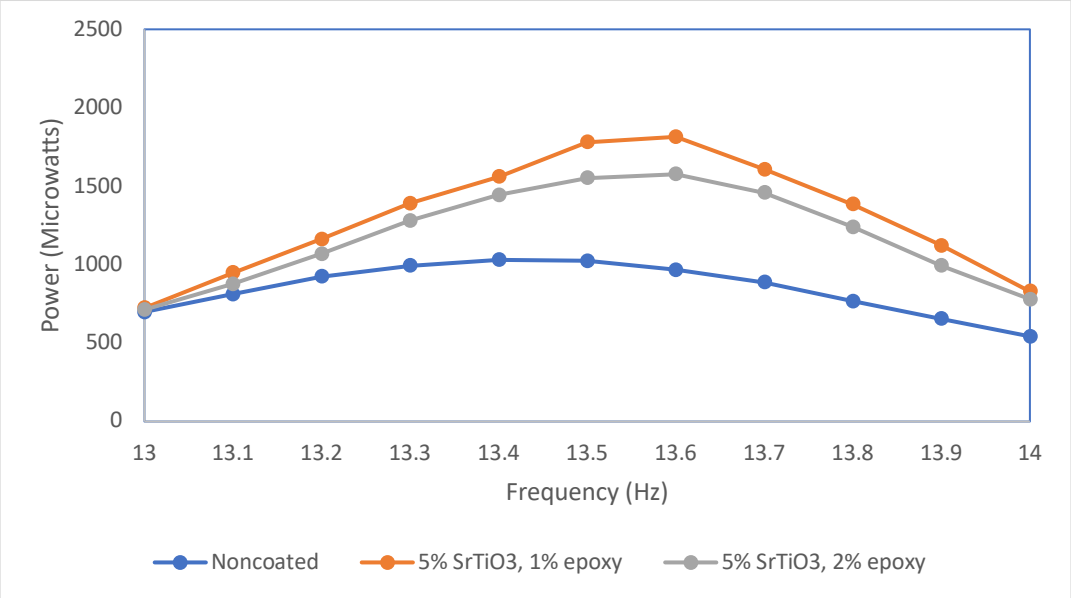

Figure 31: 5% Strontium Titanate v. Noncoated PZT

Figure 32 shows the power outputs of the composition of 10% strontium titanate with 1% epoxy and 2% epoxy as well as the noncoated PZT. At the peak power, the composition of 10% strontium titanate with 1% epoxy's power output performed 45% (efficiency value of 1.45) better than the noncoated. The peak power of the 10% strontium titanate with 2% epoxy decreased the efficiency of the PZT. It performed at an efficiency value of 0.46 of the PZT which is 54% lower.

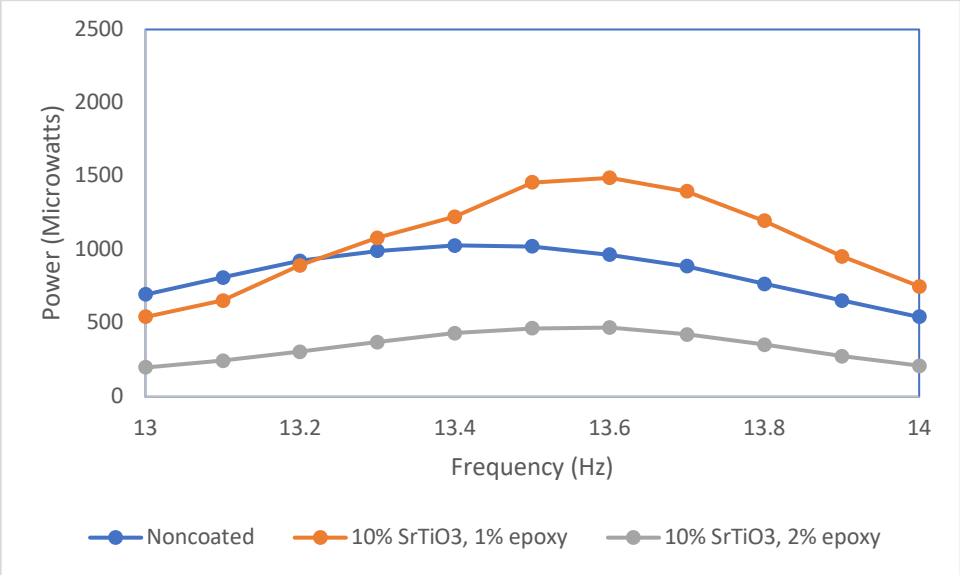

Figure 32: 10% Strontium Titanate v. Noncoated PZT

Figure 33 shows the power outputs of the composition of 15% strontium titanate with 1% and the noncoated PZT. At the peak power, the composition of 15% strontium titanate with 1% epoxy's power output performed 29% (efficiency value of 1.29) better than the noncoated. The peak power of the 15% strontium titanate with 2% epoxy enhanced the efficiency of the PZT. It performed at an efficiency value of 1.41 of the PZT which made it's performace 41% greater than the PZT.

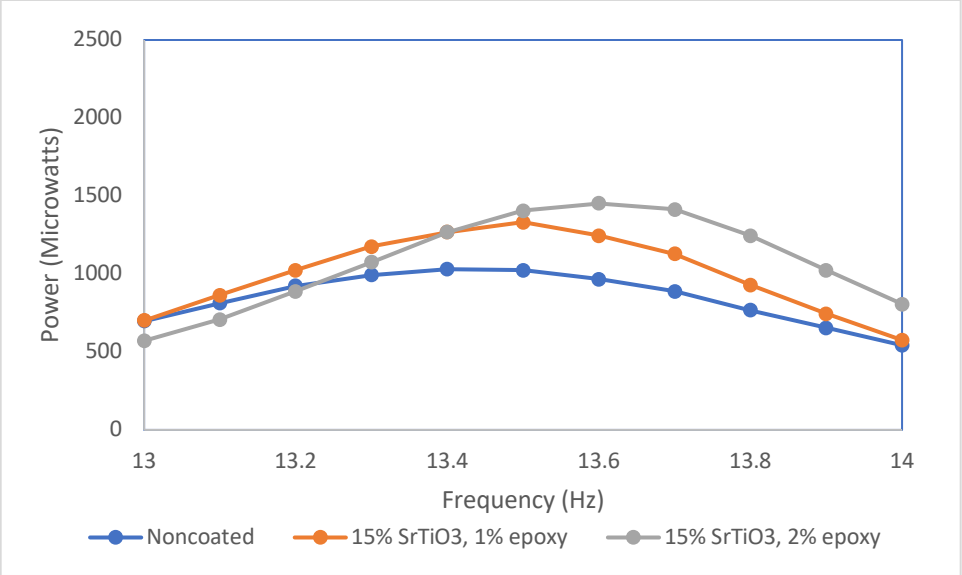

Figure 33: 15% Strontium Titanate v. Noncoated PZT

Figure 34 shows the power outputs of the composition of 20% strontium titanate with 1% epoxy and 2% epoxy as well as the noncoated PZT. At the peak power, the composition of 20% strontium titanate with 1% epoxy's power output performed 29% (efficiency value of 1.29) better than the noncoated. The peak power of the 20% strontium titanate with 2% epoxy enhanced the efficiency of the PZT. It performed at an efficiency value of 2.06 of the PZT which made its performance value 206% greater than the PZT.

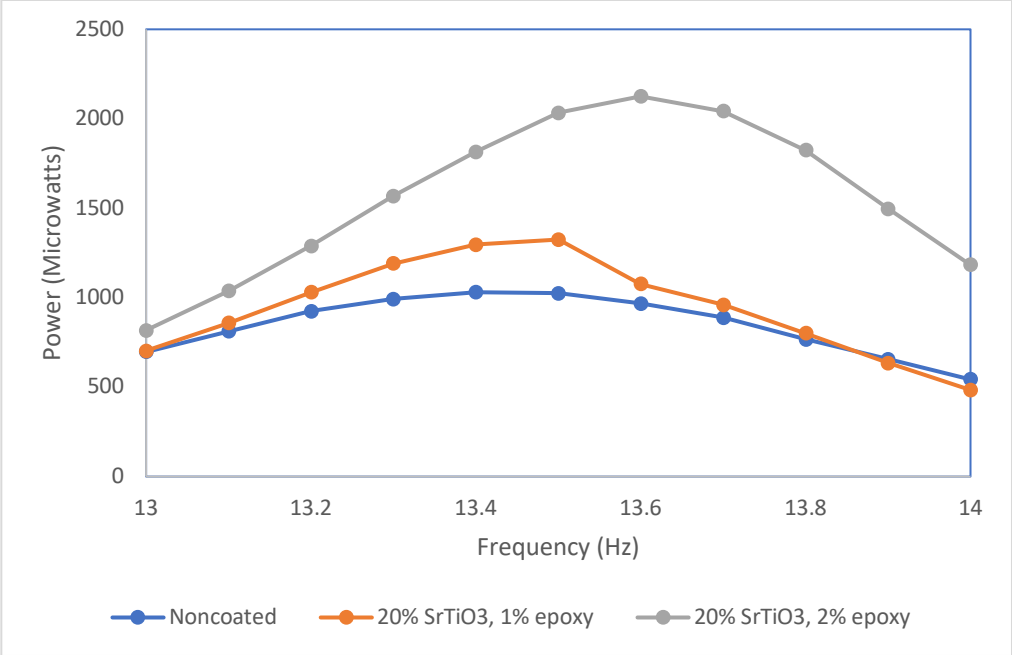

Figure 34: 20% Strontium Titanate v. Noncoated PZT

Figure 35 shows the power outputs of the composition of 30% strontium titanate with 1% epoxy and 2% epoxy as well as the noncoated PZT. At the peak power, the composition of 30% strontium titanate with 1% epoxy has a power reduction of 33% (efficiency value of 0.67) of the noncoated PZT. The peak power of the 30% strontium titanate with 2% epoxy enhanced the efficiency of the PZT. It performed at an efficiency value of 1.58 of the PZT which made its performace 158% greater than the PZT.

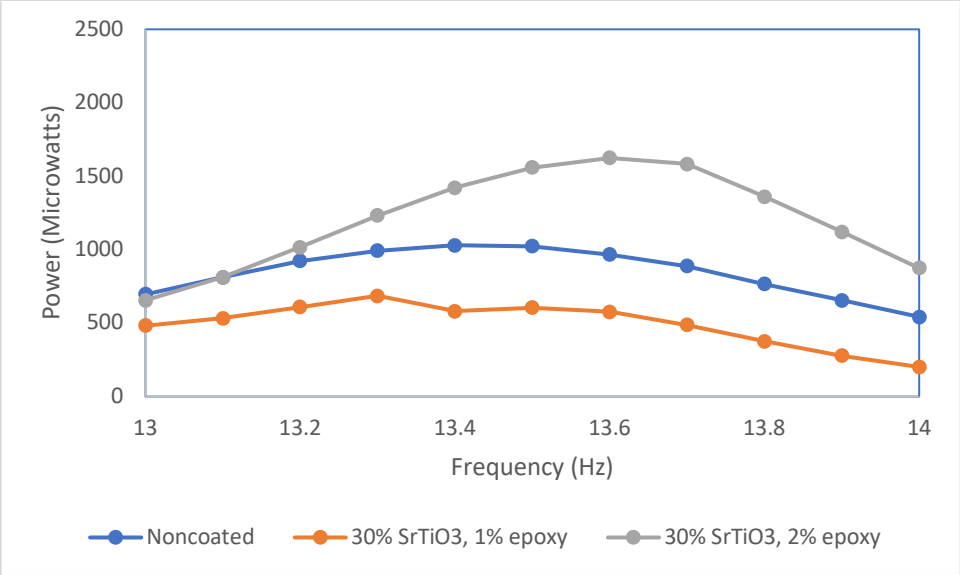

Figure 35: 30% Strontium Titanate v. Noncoated PZT

Figure 36 shows the power outputs of the composition of 40% strontium titanate with 1% epoxy and 2% epoxy as well as the noncoated PZT. At the peak power, the composition of 40% strontium titanate with 1% epoxy's power performed 72% (efficiency value of 1.72) better than the noncoated PZT. The peak power of the 40% strontium titanate with 2% epoxy enhanced the efficiency of the PZT. It performed at an efficiency value of 1.26 of the PZT which made its performace 126% greater than the PZT.

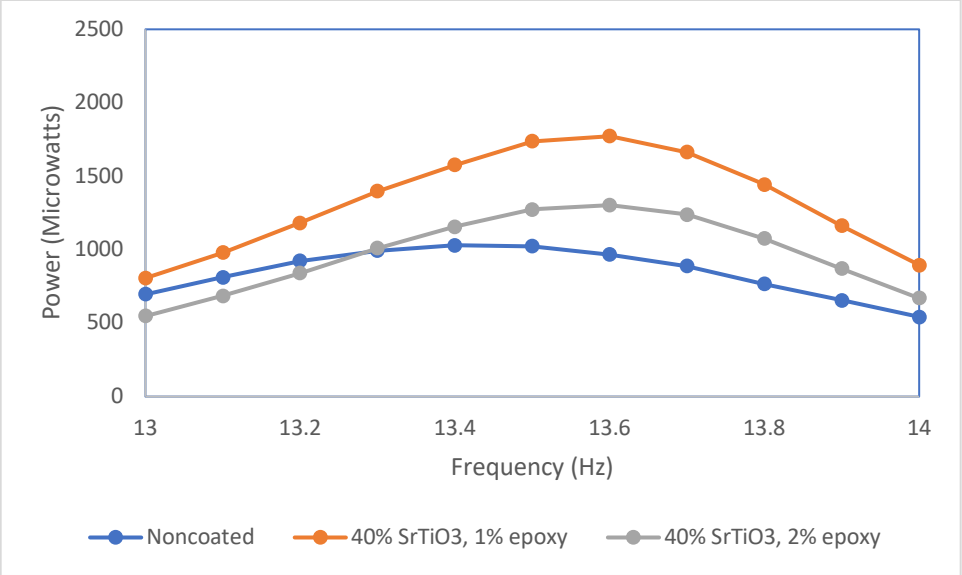

Figure 36: 40% Strontium Titanate v. Noncoated PZT

Figure 37 shows the power outputs of the composition of 60% strontium titanate with 1% epoxy and 2% epoxy as well as the noncoated PZT. At the peak power, the composition of 60% strontium titanate with 1% epoxy's power performed 66% (efficiency value of 1.66) better than the noncoated PZT. The peak power of the 60% strontium titanate with 2% epoxy enhanced the efficiency of the PZT. It performed at an efficiency value of 1.36 of the PZT which made its performance 136% greater than the PZT.

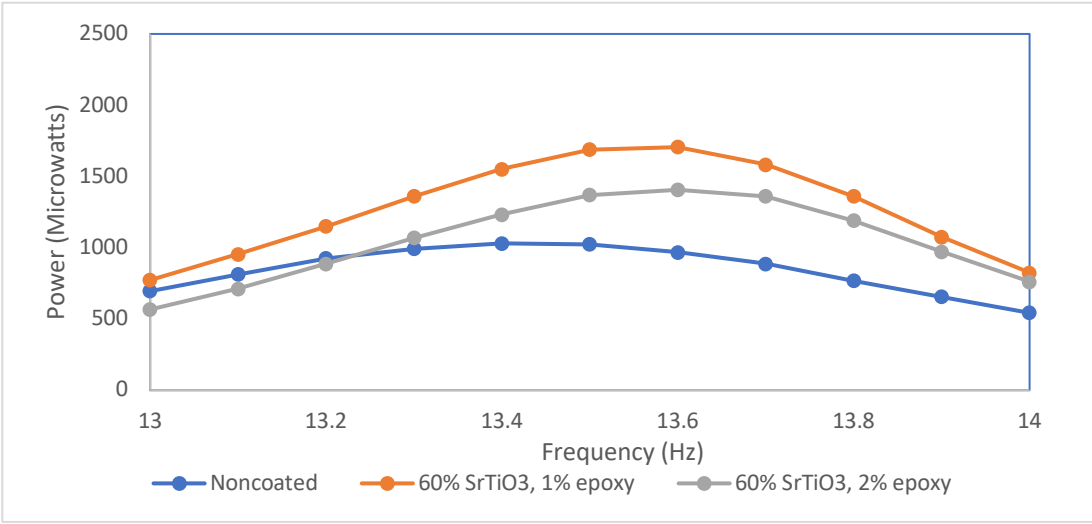

Figure 37: 60% Strontium Titanate v. Noncoated PZT

4.6 MAXIMUM POWER OUTPUT COMPARISON

To clearly see which coating combination performed the best, the top result from each combination was plotted together. This can be seen in Figure 38. The noncoated piezoelectric disk and 10% barium titanate + 2% epoxy reached their peak powers at 13.4 hertz while the other four coatings reached their peak power at 13.6 hertz.

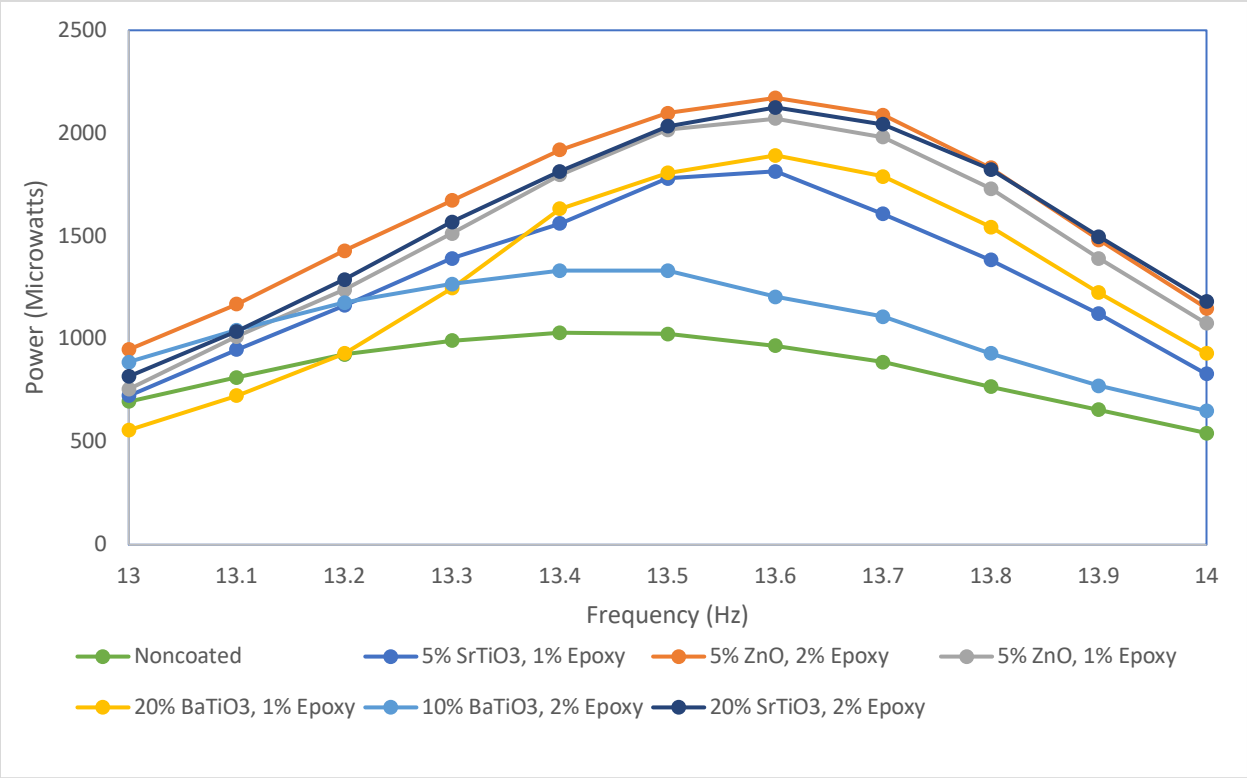

Figure 38: Maximum Power Comparison

Table 12 breaks down the graph in Figure 38 and shows the maximum power each coating was able to produce. Using this information, the relative power percentage can be found by comparing it to the peak power of the noncoated piezoceramic. The relative percentage can be fonud by using equation 10.

$$Relative\ Percentage\ = \frac{x}{x_{reference}}(100\%) \qquad (10)$$

Table 12: Peak Power

Coating	Peak Power (Microwatts)	Relative Percentage (%)
5% ZnO, 2% Epoxy	2171.56	210.75
20% SrTiO3, 2% Epoxy	2125.21	206.25
5% ZnO, 1% Epoxy	2070.25	200.92
20% BaTiO3, 1% Epoxy	1892.25	183.64
5% SrTiO3, 1% Epoxy	1814.76	176.61
10% BaTiO3, 2% Epoxy	1332.25	129.29
Noncoated	1030.41	100

4.7 COST EFFECTIVENESS

Knowing the cost of each nanoparticle, it is possible to determine which powder is the most cost efficient in terms of the power output per dollar. The cost effectiveness is calculated using equation 11, which relates how many coatings can be applied per total grams of the solution to the amount of powder to buy with respect to its price.

$$Cost\ Effectiveness = \frac{8 * Peak\ Power}{Solution} \frac{Qty}{Price} \qquad (11)$$

Where 8 is the number of disks that can have a coating applied to it in the current set up. The peak power will consist of the highest power output from the three nanopowders with no regards towards the percentage of binder resin. The solution will be the percentage of the nanoparticle used from the total weight of the solution. The total weight used was a constant 4 grams. The quantity and price can be found from the company's website. TPL, inc. was the company used to buy the barium titanate and strontium titanate, and Sigma-Aldrich was the company used to buy the zinc oxide. Table 13 contains the price and quantity of each nanopowder. The values in Table 13 will be used in equation 11.

Table 13: Nanopowders

Nanopowder	Quantity (grams)	Price ($)
Zinc Oxide	50	80.50
Barium Titanate	100	75
Strontium Titante	100	75

From Table 12, the nanopowders used in calculating the cost analysis will be 5% zinc oxide + 2% epoxy, 20% barium titanate + 1% epoxy, and 20% strontium titanate + 2% epoxy. Table 14 will contain the cost effectiveness results of each coating. This means that it will show the how much power you can get out of each coating per dollar spent on the nanoparticle.

Table 14: Cost Effectiveness

Coating	Cost Effectiveness (Microwatts/$)
5% zinc oxide + 2% epoxy	53951.80
20% barium titanate + 1% epoxy	25230
20% strontium titanate + 2% epoxy	28336.13

Figure 39 is a bar graph which is using the data from Table 14. It presents a more visualized comparison of the cost effectiveness of the selected nanoparticle coatings.

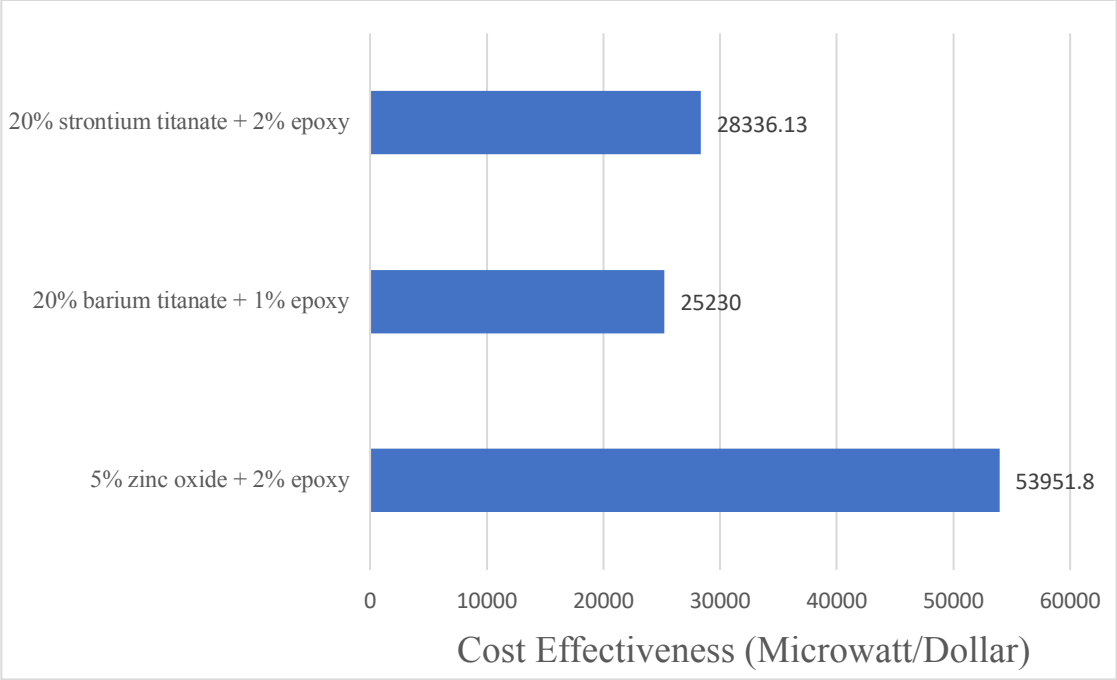

Figure 39: Nanoparticle Cost Effectiveness

4.8 RELATIVE PERCENTAGE

Figure 40 shows the relative percentage of each mixture compared to the noncoated ceramic piezoelectric. The percent mixture is the percentage of nanoparticle used to make each coating mixture while the relative change is the ratio of the coated material to the noncoated. If the relative change is above 1, this means that the specific coating mixture enhanced the piezoelectric. It can be seen that both zinc oxide compositions tend to stay above one while the other compositions fall below one at some point. Equation 6 was used in order to calculate the relative percentage.

Various factors can be applied for why the data's outcome results this way, such as the ceramic could have been affected by the nanoparticle composition, how it was spin coated, or even the vibration source.

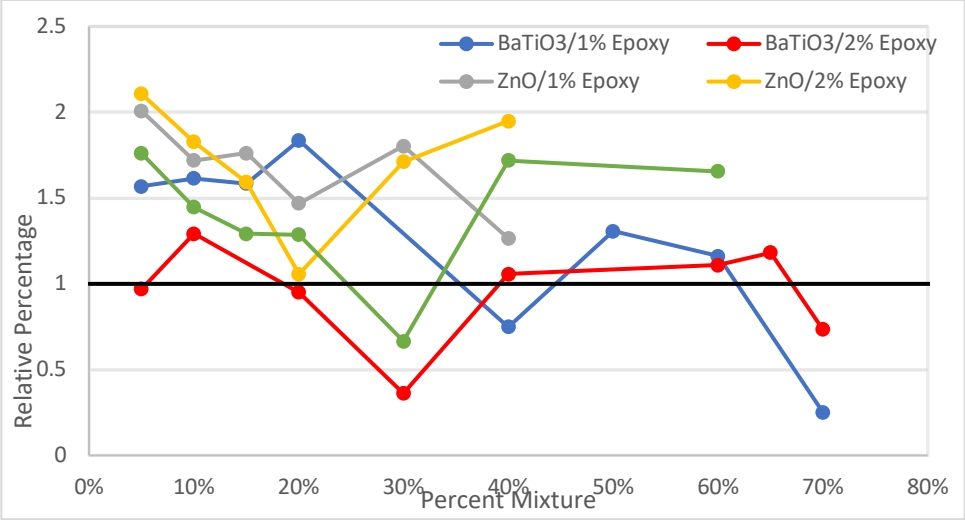

Figure 40: Relative Percentage

4.9 PRACTICAL APPLICATIONS

At the moment, harvesting energy through vibrations is applicable through low energy systems. The piezoelectric ceramic can be installed in the bottom of shoes and be utilized to store charges in a capacitor or battery. This energy can then be used to power devices such as a cellular phone or other handheld accessories. The piezoelectric can also be applied to harvest energy from vehicles due to the continuous vibrations when the vehicle is running and from pavement by traffic vibration. Table 15 shows a comparison of power density between vibration and solar sources. Solar cell's power density is about forty times greater than vibration which means that for the vibration source to replace the solar source it would need 69,000 disks and an area of 39.51 meters to harvest the same power. It is possible, however, for both sources to coexist and work together in case the solar source malfunctions due to lack of sunlight, rain and cloudy weather, snowy day, or if it is being replaced after its useful life.

Table 15: Power Density

Energy Source	Power Density (W/m^2)	Equivalent Area (m^2)
Solar	150	1
Vibration	3.796	39.51

5. CONCLUSION AND FUTURE WORK

The goal of this study was to maximize the power output of a piezoelectric ceramic for a low energy system. This was done by preparing multiple mixtures and applying them as coatings to the top of the ceramic. The mixture composition contained different types of nanoparticles, ferrofluid, and an epoxy to create a bond between the ceramics and nanocoating. The optimum power output was found for each nanocoating and epoxy mixture. The optimum mixture for barium titanate consisted of 20% nanoparticles, 1% epoxy, and 79% ferrofluid. The power output for 20% barium titanate with 1% epoxy which had a value of 1892.25 microwatts and enhanced the ceramic power output by 83.64%. The optimum coating for strontium titanate consisted of 20% nanoparticles with 2% epoxy, which produced an optimum power output of 2125.21 microwatts and enhanced the ceramic power output by 106.25%. The optimum coating for zinc oxide consisted of 5% nanoparticles, 2% epoxy, and 93% ferrofluid. 5% zinc oxide with 2% epoxy resulted in having the highest peak power output of 2171.56 microwatts and enhanced the ceramic by 110.75%. The cost effectiveness was found to determine which nanopowder had the best performance for their dollar. 20% barium titanate with 1% epoxy has the lowest power output per dollar being 25230 microwatts per dollar. 5% zinc oxide with 2% epoxy had a cost effectiveness of 53951.80 microwatts per dollar. 20% strontium titanate with 2% epoxy had a cost analysis of 28336.13 microwatts per dollar. It can be stated that the mixture containing 5% zinc oxide with 2% epoxy is the best choice if money is a major factor as well as enhancing the power output of a traditional PZT ceramic.

5.1 FUTURE WORK

For future work, suggestions can be made to optimize the geometry of the plate. Instead of using a beam, the piezoelectric ceramic could be set on something that utilizes the whole area of the ceramic. Establish the impact of the percentage of epoxy for a particular ceramic on power output. It would be beneficial to consider utilizing plasma etching to improve the power output of the system. In order to characterize the coating, the use of a Scan Electron Microscope should be utilized. Lastly, testing of the coated PZTs should be applied in the field of energy harvesting.

REFERENCES

[1] Mantena, P. Raju. “ME 416 Structures and Dynamics Laboratory”. Lab handbook. The University of Mississippi. Oxford. Fall 2014. Print.
[2] Jaffe, B., Cook, & Jaffe, H. “Historical Introduction.” Piezoelectric Ceramics. Academic Press Inc. London and New York. 1971. 1-6. Print.
[3] Jaffe, B., Cook, & Jaffe, H. “The Piezoelectric Effect in Ceramics.” Piezoelectric Ceramics. Academic Press Inc. London and New York. 1971. 7-22. Print.
[4] Jaffe, B., Cook, & Jaffe, H. “The Perovskite Structure.” Piezoelectric Ceramics. Academic Press Inc. London and New York. 1971. 49-52. Print.
[5] Jaffe, B., Cook, & Jaffe, H. “Barium Titanate.” Piezoelectric Ceramics. Academic Press Inc. London and New York. 1971. 53-114. Print.
[6] Lucena, R., et al. “Potential of Nanoparticles in Sample Preparation.” Journal of Chromatography A, vol. 1218, no. 4, 2011, pp. 620-637.
[7] Raj, Moskowitz, and Casciari. “Advances in ferrofluid technology.” Journal of Magnetism and Magnetic Materials, vol. 149, no. 1-2, 1995, pp. 174-180.
[8] Wang, Zhong Lin, and Wenzhuo Wu. “Nanotechnology-Enabled Energy Harvesting for Self-Powered Micro-/Nanosystems.” Angewandte Chemie International Edition, vol. 51, no. 47, Apr. 2012, pp. 11700–11721., doi:10.1002/anie.201201656.
[9] Williams, C.b., and R.b. Yates. “Analysis of a Micro-Electric Generator for Microsystems.”Sensors and Actuators A: Physical, vol. 52, no. 1-3, 1996, pp. 8–11
[10] Fang, Hua-Bin, et al. “Fabrication and Performance of MEMS-Based Piezoelectric Power Generator for Vibration Energy Harvesting.” Microelectronics Journal, vol. 37, no. 11, 2006, pp. 1280–1284.
[11] Priya, Shashank and Inman, Daniel. “Piezoelectric Energy Harvesting.” Energy Harvesting Technologies. Springer. pp. 3-36.
[12] Kim, H., Kim, JH., & Kim, J. “A Review of Piezoelectric Energy Harvesting Based on Vibration.” International Journal of Precision Engineering and Manufacturing, vol. 12, no. 6, pp. 1129-1141.
[13] Caliò², Renato, et al. “Piezoelectric Energy Harvesting Solutions.” Sensors, vol. 14, no. 3, Oct. 2014, pp. 4755–4790.
[14] Ottman, G.k., et al. “Adaptive Piezoelectric Energy Harvesting Circuit for Wireless Remote Power Supply.” IEEE Transactions on Power Electronics, vol. 17, no. 5, 2002, pp. 669–676., doi:10.1109/tpel.2002.802194.
[15] Le, T.t., et al. “Piezoelectric Micro-Power Generation Interface Circuits.” IEEE Journal of Solid-State Circuits, vol. 41, no. 6, 2006, pp. 1411–1420., doi:10.1109/jssc.2006.874286.
[16] Beeby, S P, et al. “Energy Harvesting Vibration Sources for Microsystems Applications.”Measurement Science and Technology, vol. 17, no. 12, 2006, doi:10.1088/0957-0233/17/12/r01.
[17] Platt, S.r., et al. “On Low-Frequency Electric Power Generation With PZT Ceramics.”IEEE/ASME Transactions on Mechatronics, vol. 10, no. 2, 2005, pp. 240–252., doi:10.1109/tmech.2005.844704.
[18] Jordan, T. L., and Zoubeida Ounaies. Piezoelectric Ceramics Characterization. National Aeronautics and Space Administration, Langley Research Center, 2001.
[19] Linz, Arthur. “Some Electrical Properties of Strontium Titanate.” Physical Review, vol. 91, no. 3, Jan. 1953, pp. 753–754., doi:10.1103/physrev.91.753.2.

[20] Saifi, M. A., and L. E. Cross. “Dielectric Properties of Strontium Titanate at Low Temperature.” Physical Review B, vol. 2, no. 3, Jan. 1970, pp. 677–684., doi:10.1103/physrevb.2.677.
[21] Kim, Minsoo, et al. “Synthesis of Strontium Titanate Nanoparticles Using Supercritical Water.”Ceramics International, vol. 42, no. 15, 2016, pp. 17853–17857., doi:10.1016/j.ceramint.2016.08.120.
[22] Cowley, R. A. “Lattice Dynamics and Phase Transitions of Strontium Titanate.” Physical Review, vol. 134, no. 4A, 1964, doi:10.1103/physrev.134.a981.
[23] Balachandran, U., and N.g. Eror. “Electrical Conductivity in Strontium Titanate.” Journal of Solid State Chemistry, vol. 39, no. 3, 1981, pp. 351–359., doi:10.1016/0022-4596(81)90270-x.
[24] Hall, David B., et al. “Spin Coating of Thin and Ultrathin Polymer Films.” Polymer Engineering & Science, vol. 38, no. 12, 1998, pp. 2039–2045., doi:10.1002/pen.10373.
[25] Flack, Warren W., et al. “A Mathematical Model for Spin Coating of Polymer Resists.” Journal of Applied Physics, vol. 56, no. 4, 1984, pp. 1199–1206., doi:10.1063/1.334049.
[26] Emslie, Alfred G., et al. “Flow of a Viscous Liquid on a Rotating Disk.” Journal of Applied Physics, vol. 29, no. 5, 1958, pp. 858–862., doi:10.1063/1.1723300.
[27] Lawrence, C. J. “The Mechanics of Spin Coating of Polymer Films.” Physics of Fluids, vol. 31, no. 10, 1988, p. 2786., doi:10.1063/1.866986.
[28] Platt, S.r., et al. “The Use of Piezoelectric Ceramics for Electric Power Generation Within Orthopedic Implants.” IEEE/ASME Transactions on Mechatronics, vol. 10, no. 4, 2005, pp. 455–461., doi:10.1109/tmech.2005.852482.
[29] Takenaka, Tadashi, and Hajime Nagata. “Current Status and Prospects of Lead-Free Piezoelectric Ceramics.” Journal of the European Ceramic Society, vol. 25, no. 12, 2005, pp. 2693–2700., doi:10.1016/j.jeurceramsoc.2005.03.125.
[30] Kim, Hyeoungwoo, et al. “Consideration of Impedance Matching Techniques for Efficient Piezoelectric Energy Harvesting.” IEEE Transactions on Ultrasonics, Ferroelectrics and Frequency Control, vol. 54, no. 9, 2007, pp. 1851–1859., doi:10.1109/tuffc.2007.469.
[31] Elvin, Niell G., and Alex A. Elvin. “A General Equivalent Circuit Model for Piezoelectric Generators.” Journal of Intelligent Material Systems and Structures, vol. 20, no. 1, 2008, pp. 3–9., doi:10.1177/1045389x08089957.
[32] Cady, W.g. “The Piezo-Electric Resonator.” Proceedings of the IRE, vol. 10, no. 2, 1922, pp. 83–114., doi:10.1109/jrproc.1922.219800.
[33] Richter, BjÃ¶rn, et al. “Piezoelectric Equivalent Circuit Models.” Energy Harvesting Technologies, pp. 107–128., doi:10.1007/978-0-387-76464-1_4.
[34] Kokkinopoulos, A., et al. “Energy Harvesting Implementing Embedded Piezoelectric Generators – The Potential for the Attiki Odos Traffic Grid.” *Energy Procedia*, vol. 50, 2014, pp. 1070-1085., doi:10.1016/j.egypro.2014.06.126.
[35] Li, Xiaofeng, and Vladimr Strezov. “Modelling Piezoelectric Energy Harvesting Potential in an Educational Building.” *Energy Conversion and Management*, vol. 85, 2014, pp. 435-442., doi:10.1016/j.enconman.2014.05.096
[36] Ryall, Julian. 12 Dec. 2008, “Japan harnesses energy from footsteps,” from http://www.telegraph.co.uk/news/earth/energy/3721841/Japan-harnesses-energy-from-footsteps.html
[37] Murata Manufacturing Co. 1 Aug. 1978, *7BB-27-4KL0.* Retrieved from https://www.murata.com/en-us/products/productdetail?partno=7BB-27-4L0

[38] Anton, Steven R., and Henry A. Sodano. "A Review of Power Harvesting using Piezoelectric Materials (2003–2006)." *Smart Materials and Structures*, vol. 16, no. 3, 2007, pp. R1-R21.
[39] Sharma, Sudhanshu. "Smart Nanocoated Structure for Energy Harvesting at Low Frequency Vibration." Dissertation, The University of Mississippi, May 2012.

APPENDICES

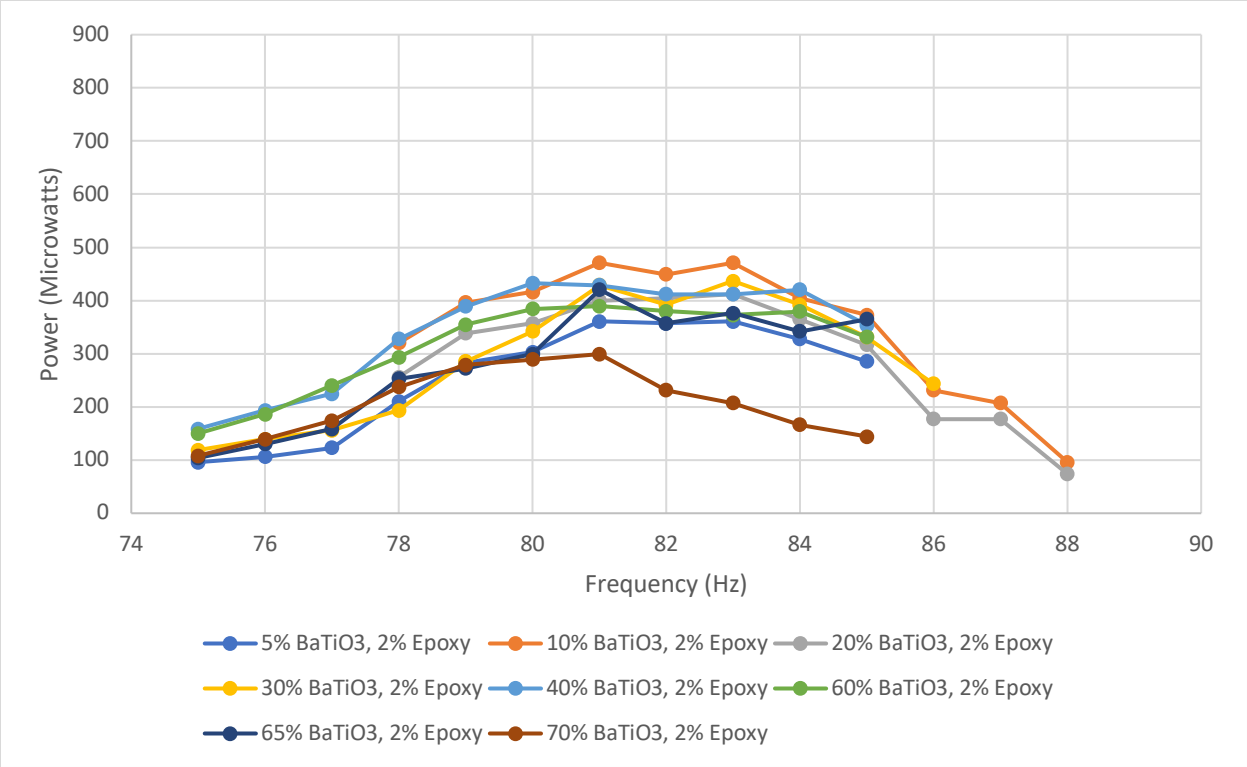

Figure 41: BaTiO3 w/2% Epoxy v. Frequency (2nd Mode)

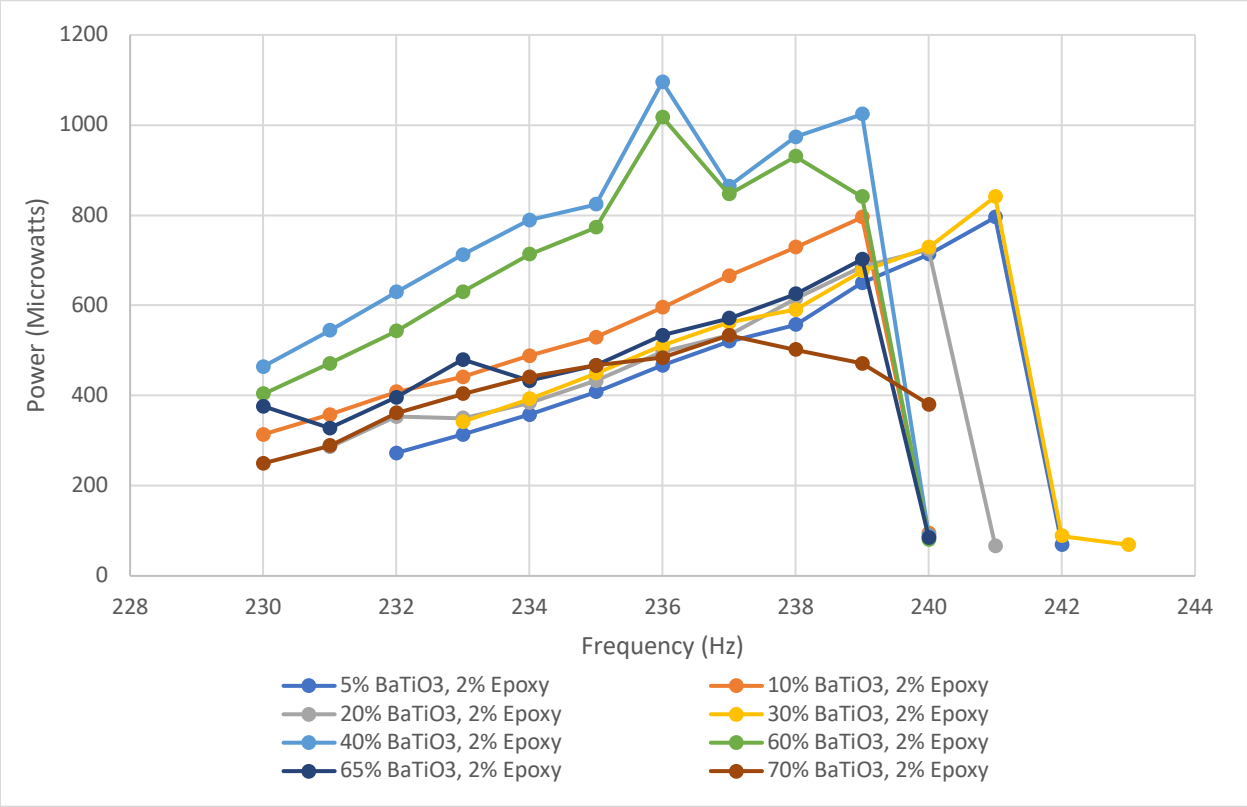

Figure 42: BaTiO3 w/2% Epoxy v. Frequency (3rd Mode)

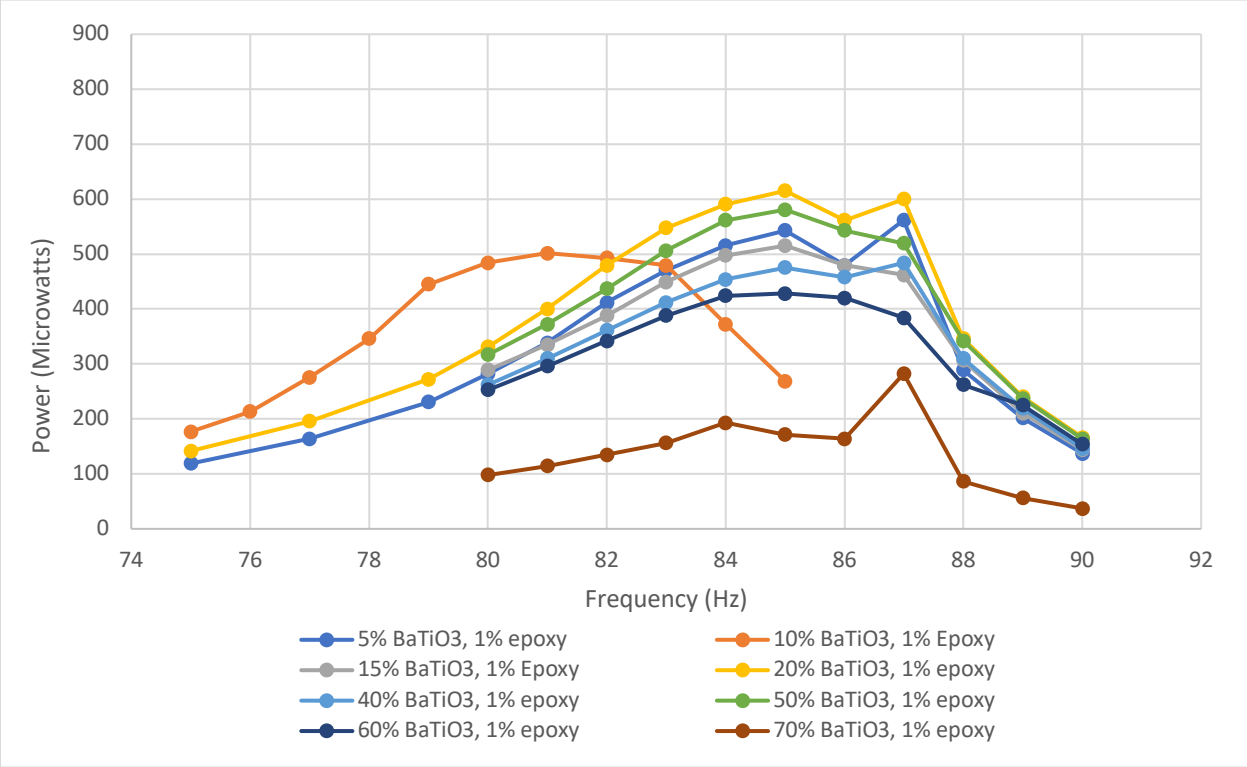

Figure 43: BaTiO3 w/1% Epoxy v. Frequency (2nd Mode)

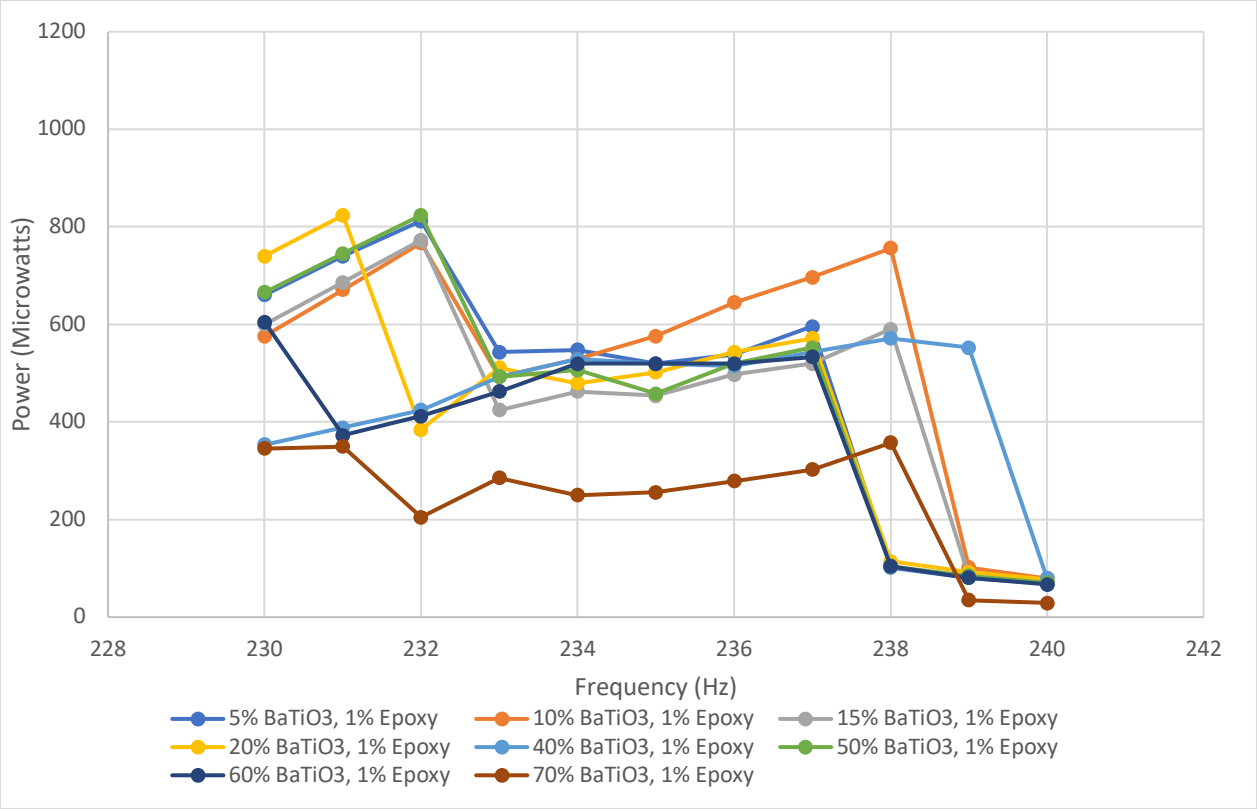

Figure 44: BaTiO3 w/1% Epoxy v. Frequency (3rd Mode)

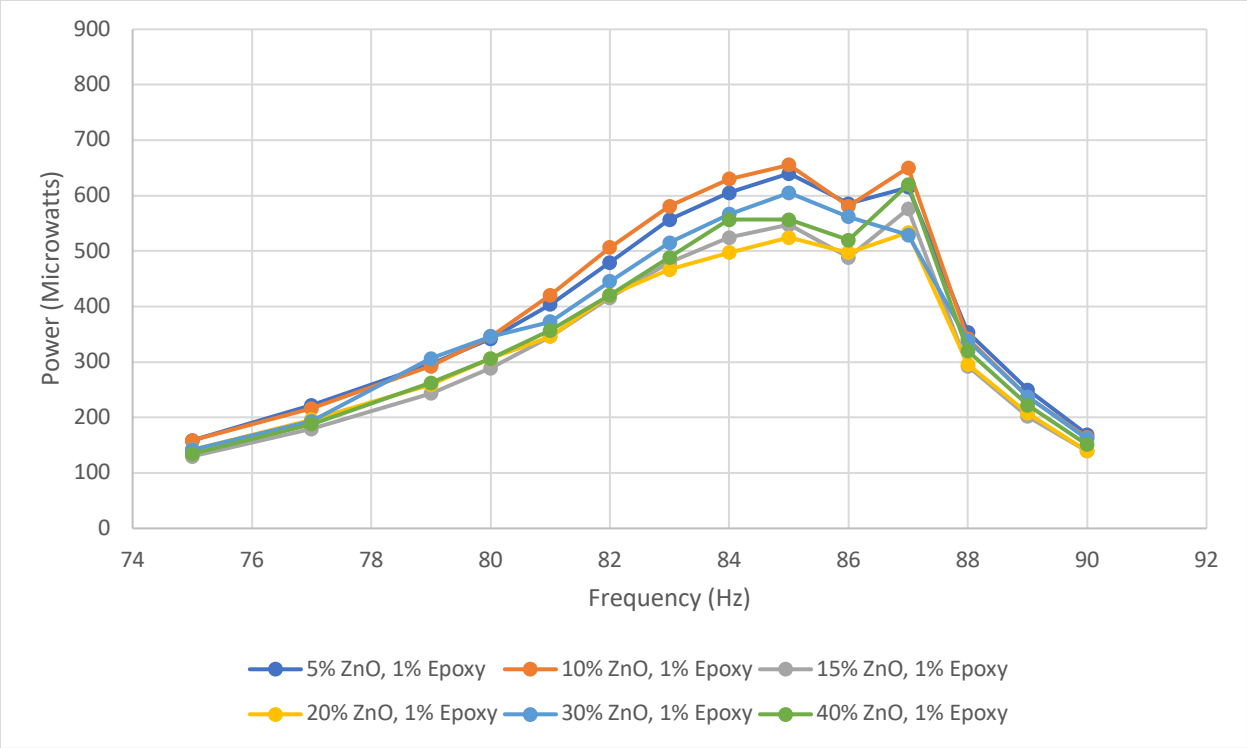

Figure 45: ZnO w/1% Epoxy v. Frequency (2nd Mode)

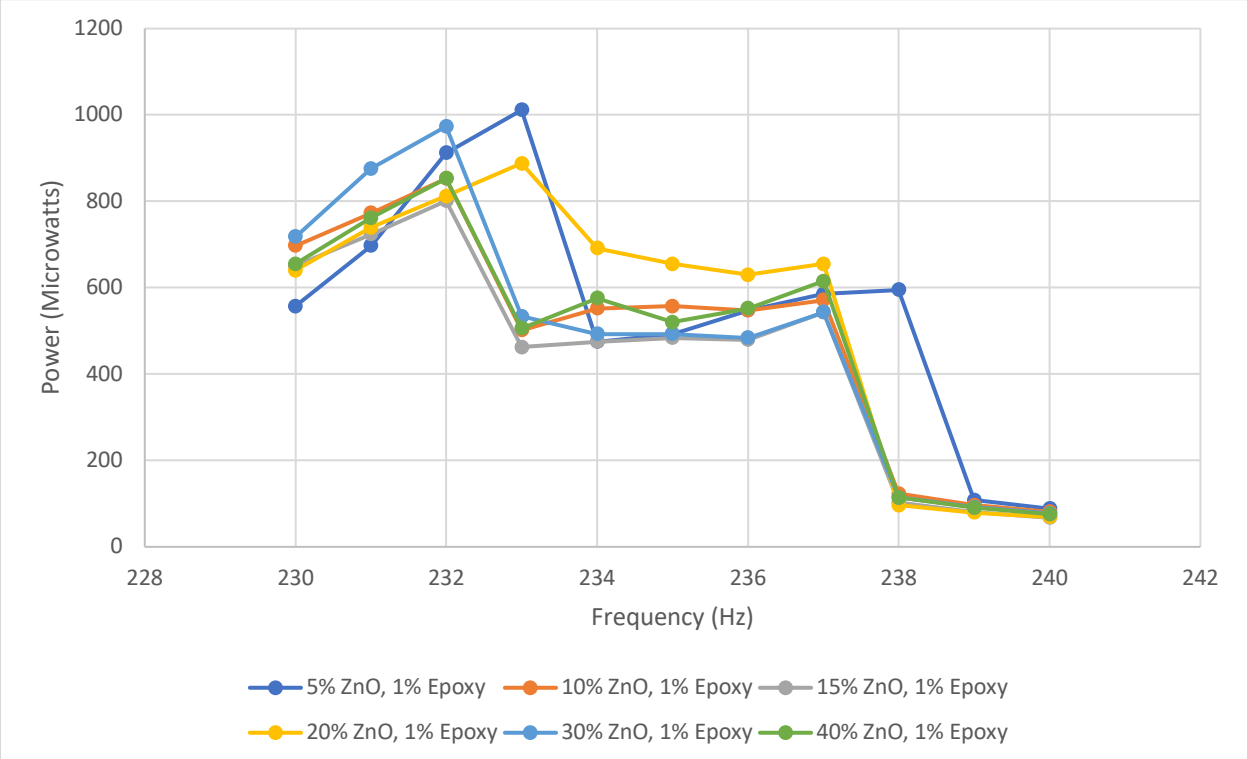

Figure 46: ZnO w/1% Epoxy v. Frequency (3rd Mode)

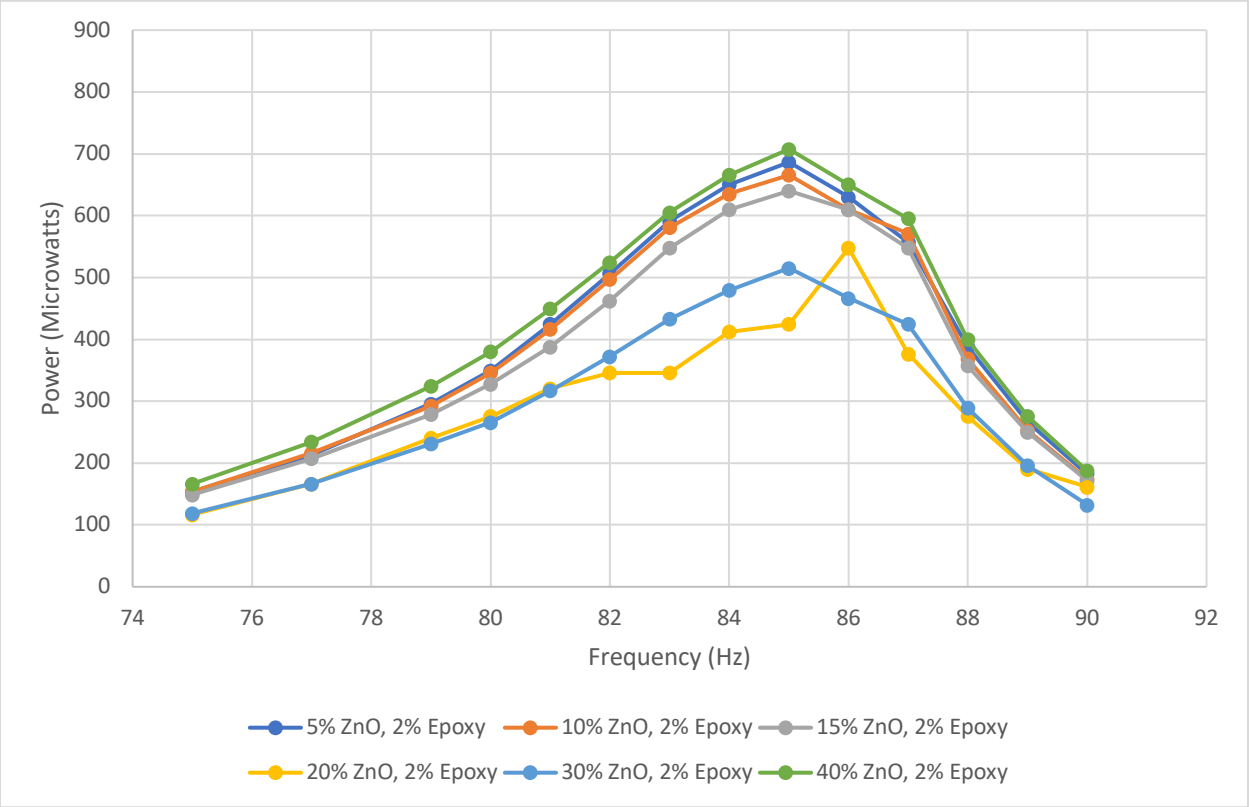

Figure 47: ZnO w/2% Epoxy v. Frequency (2nd Mode)

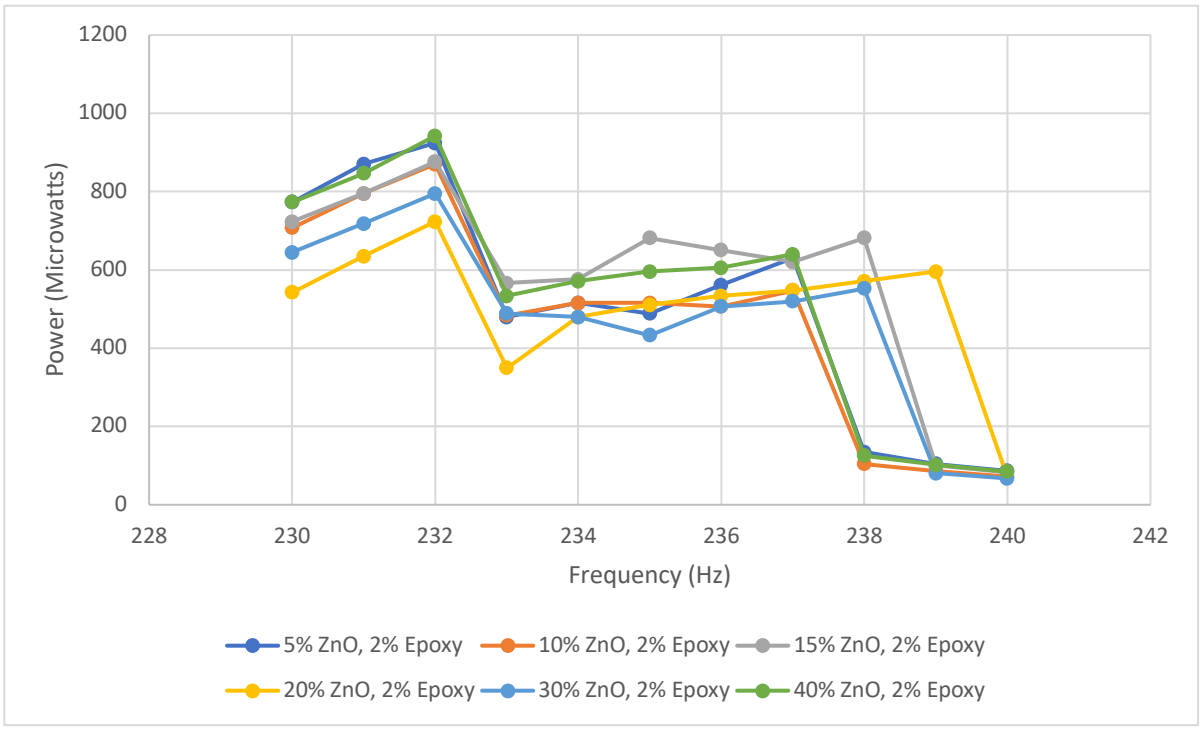

Figure 48: ZnO w/2% Epoxy v. Frequency (3rd Mode)

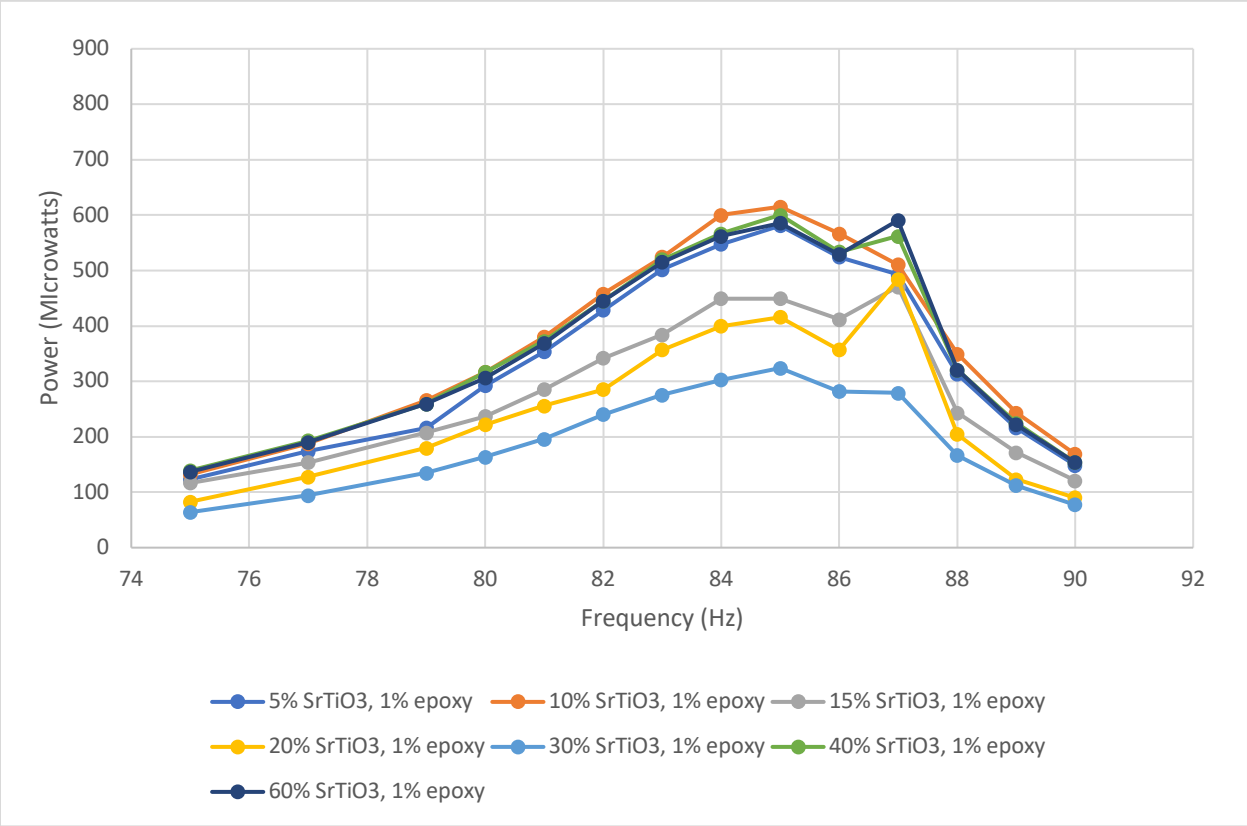

Figure 49: SrTiO3 w/1% Epoxy v. Frequency (2nd Mode)

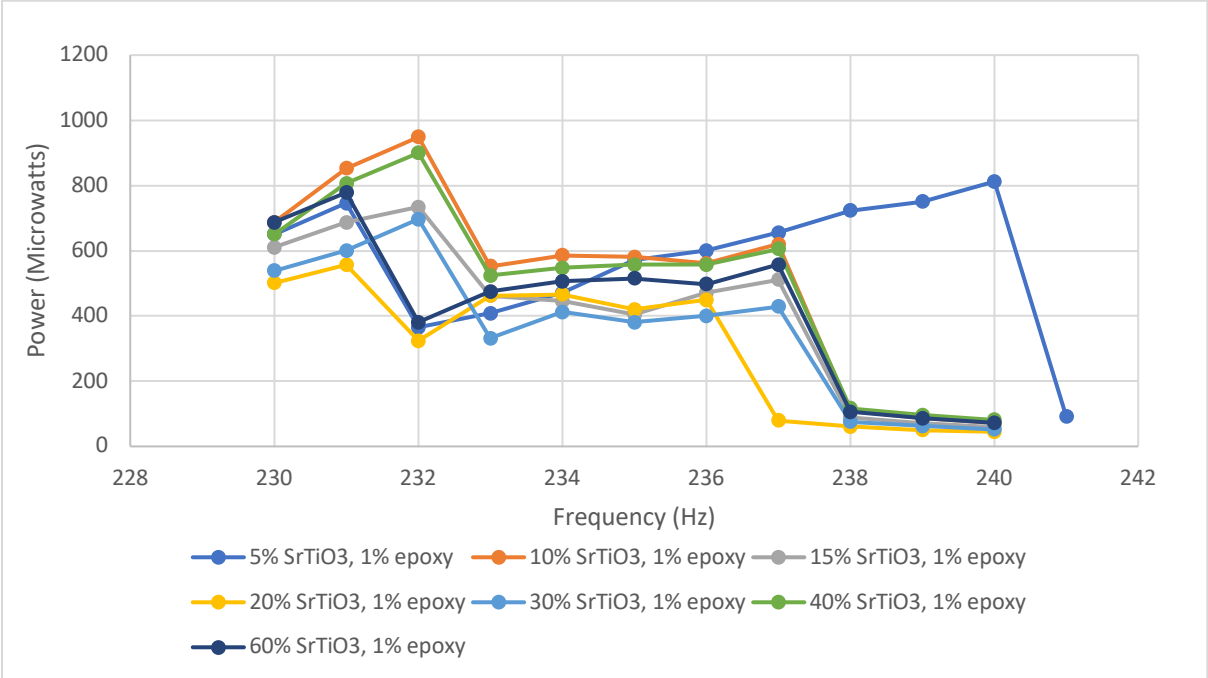

Figure 50: SrTiO3 w/1% Epoxy v. Frequency (3rd Mode)

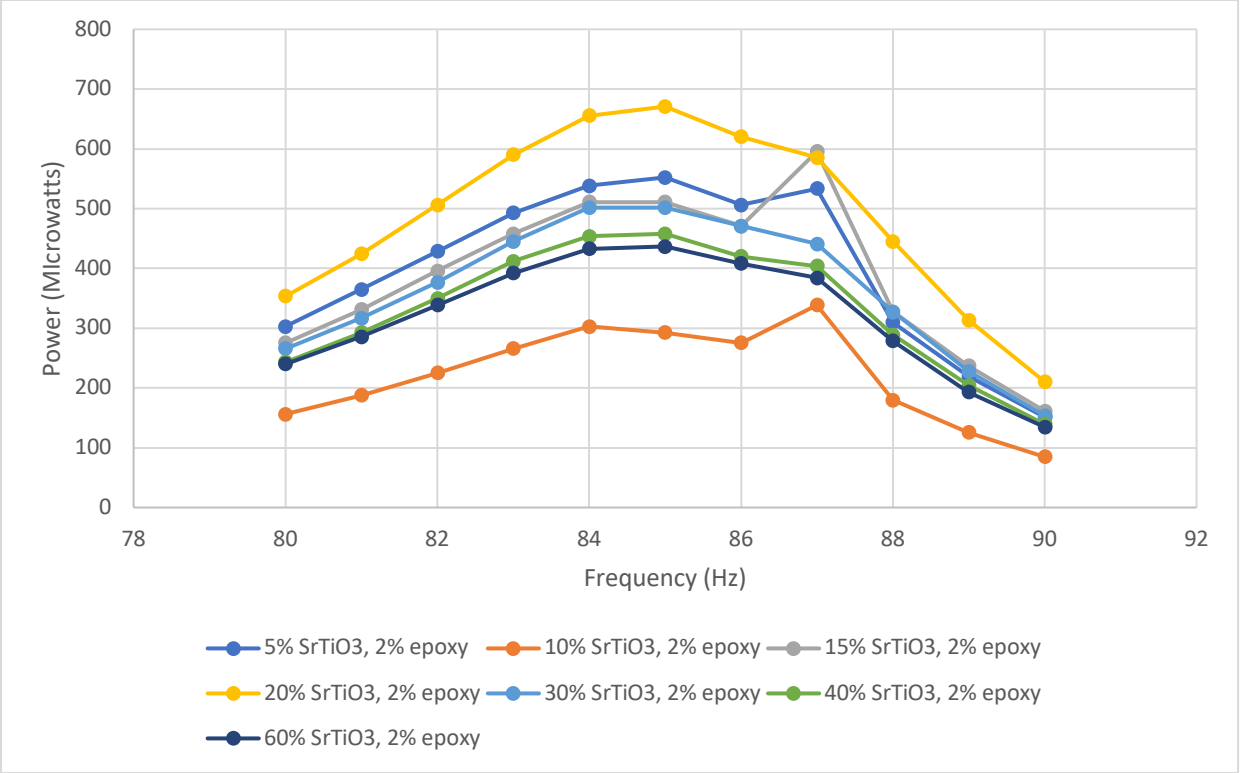

Figure 51: SrTiO3 w/ 2% Epoxy v. Frequency (2nd Mode)

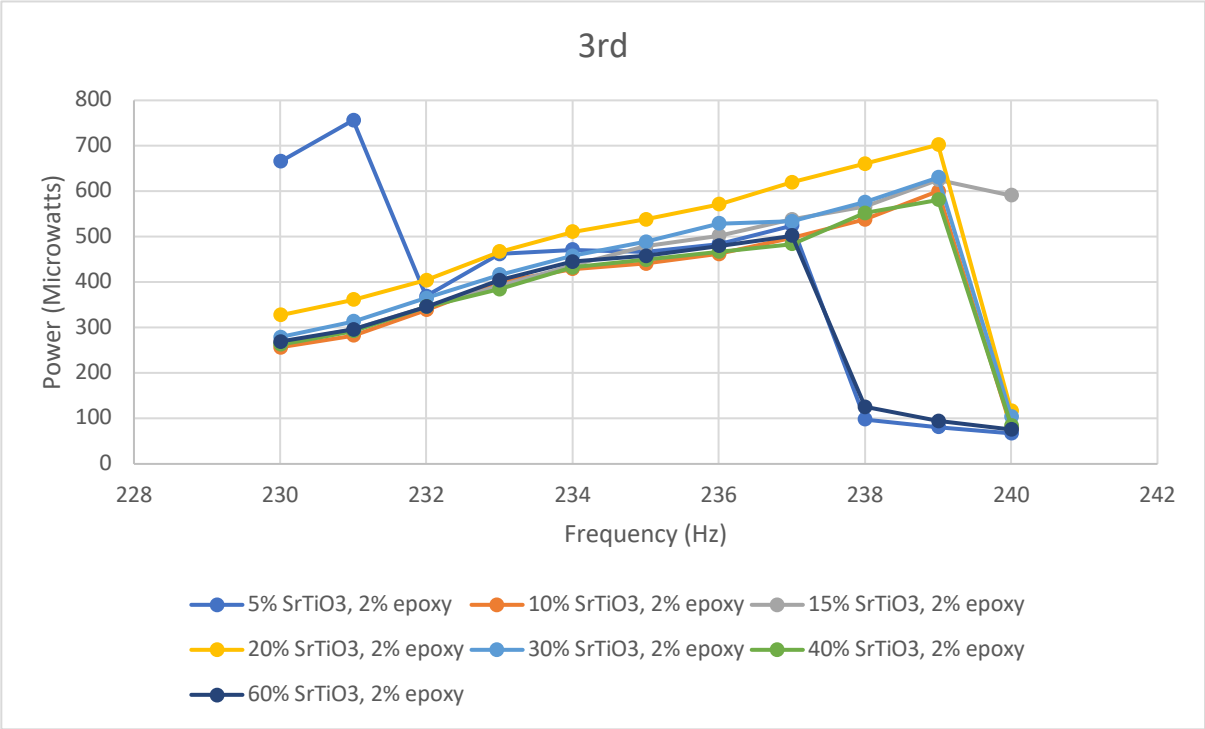

Figure 52: SrTiO3 w/ 2% Epoxy v. Frequency (3rd Mode)

VITA

Quinten Michael Humphrey, son of Mary Humphrey and David Humphrey, was born in Naples, Florida. He received his Bachelor of Science in Mechanical Engineeringfrom the University of Mississippi in May of 2015. After graduation, he continued his education at the University of Mississippi where he received his Master of Science in Engineering Science with an emphasis in Mechanical Engineering in May of 2018.